

SEISMIC ASSESSMENT AND RETROFITTING STRATEGIES FOR A
PROMINENT MASONRY STRUCTURE AFFECTED BY EARTHQUAKE

A THESIS SUBMITTED TO
THE FACULTY OF ARCHITECTURE AND ENGINEERING
OF
EPOKA UNIVERSITY

BY

JOZEFINA STERKAJ

IN PARTIAL FULFILLMENT OF THE REQUIREMENTS
FOR
THE DEGREE OF MASTER OF SCIENCE
IN
CIVIL ENGINEERING

MARCH, 2024

Approval sheet of the Thesis

This is to certify that we have read this thesis entitled “**Seismic Assessment and Retrofitting Strategies for a Prominent Masonry Structure affected by Earthquake**” and that in our opinion it is fully adequate, in scope and quality, as a thesis for the degree of Master of Science.

Assoc. Prof. Mirjam Ndini
Head of Department
Date: March, 01, 2024

Examining Committee Members:

Assoc. Prof. Mirjam Ndini (Civil Engineering) _____

Dr. Armando Demaj (Civil Engineering) _____

Dr. Marsed Leti (Civil Engineering) _____

I hereby declare that all information in this document has been obtained and presented in accordance with academic rules and ethical conduct. I also declare that, as required by these rules and conduct, I have fully cited and referenced all material and results that are not original to this work.

Name Surname: Jozefina Sterkaj

Signature: _____

ABSTRACT

Seismic Assessment and Retrofitting Strategies for a Prominent Masonry Structure affected by Earthquake

Sterkaj, Jozefina

Master of Science, Department of Civil Engineering

Supervisor: Assoc. Prof. Mirjam Ndini

In Albania, masonry is still widely used in construction. It reached its peak during the communist era (1944–1990), when structures with load-bearing stone walls were built using the Albanian Building Code (KTP) as a guide. The November 26, 2019, earthquake highlighted these structures' susceptibility to seismic activity, which calls for a careful assessment of their seismic resilience.

This study highlights the importance of modern retrofitting methods on older buildings in the protection of architectural history in areas that are vulnerable to earthquakes. An unreinforced masonry building (URM) constructed in the year 1940 in Tirana is the subject of the seismic performance evaluation. First, a thorough site examination is conducted, then samples of the masonry units are taken out of the chosen structure.

The numerical study uses a macromodelling technique with the TREMURI finite element analysis tool, including mechanical features obtained from experimental test data. According to the investigation, the URM building exhibits minimal damage and remarkable seismic resilience. This means that strengthening modifications may improve its seismic performance.

The analysis results show that the URM building suffers moderate damage under seismic loads. A post-intervention analysis to highlight the seismic performance improvements are recommended as possible future works.

The study concludes by suggesting a chosen strategie of intervention based on the damage of the structure. It is advised that future research carry out a post-intervention analysis that evaluates and highlights possible enhancements in seismic performance. This study adds to the current conversation on seismic resilience by offering insightful

information about retrofitting techniques for Albania's ancient masonry buildings, especially in light of the country's recent seismic incidents.

Keywords: *Unreinforced masonry buiding, risk assessment, finite element modelling, non-linear static analysis, seismic action, strengthening.*

ABSTRAKT

Vlerësimi Sizmik dhe Mënyrat e Përforcimit të një Objekti të Rëndësisë së Vecantë prej Murature e ndikuar nga Tërmeti

Sterkaj, Jozefina

Master I Shkencave, Departamenti i Inxhinierisë së Ndërtimit

Udhëheqësi: Assoc. Prof. Mirjam Ndini

Në Shqipëri, muratura vazhdon të përdoret gjerësisht në ndërtim. Ndërtimi me tulla arriti kulmin gjatë periudhës komuniste (1944-1990), kur projektet tip të ndërtimeve të objekteve me mure mbajtës të ngarkuara u projektuan sipas udhëzimeve të Kushtit Teknik të Projektimit (KTP). Aktiviteti i lartë sizmik i Shqipërisë vecanwrisht twrmeti i 26 nëntor 2019 tregoi dobësinë e këtyre strukturave ndaj forcave të tërmetit dhe e bëri verifikimin e rezistencës së tyre sizmike një çështje për tu marrë parasysh.

Ky studim nënvizon rëndësinë e adaptimit të teknikave moderne të riparimit për ndërtime historike, duke siguruar mbrojtjen e qëndrueshme të trashëgimisë arkitektonike në rajonet me rrezik sizmik. Një ndërtesë me murë të papërforcuar (URM) e ndërtuar në Tiranë në vitin 1940, ajo është përzgjedhur nga stoku I ndërtimeve dhe i është nënshtruar një vlerësimi seizmik të performances. Procesi fillon me një hetim në vendin e ndërtimit, ku merren mostra të njësive të murit nga ndërtesa e studiuar. Teste eksperimentale kryhen sipas rregullores ASTM C67-09, ku përcaktohen pronat e materialeve të njësive të murit. Programi analitik me elemente të kufizuara TREMURI përdoret për fazën e analizës numerike. Ndërtesa modelohet duke përdorur qasjen e makromodelimit dhe karakteristikat mekanike të murit merren nga rezultatet e testeve eksperimentale.

Rezultatet e analizës tregojnë se ndërtesa URM shfaq një rezistencë sismike të ulët duke treguar dëme të moderuara, kështu që çdo ndërhyrje për forcim mund të jetë e mundur. Në fund, prezantohen një teknike ndërhyrjeje, më e përdorura gjatë këtyre viteve në vendin tonë. Rekomandohet një analizë pas-ndërhyrje për të theksuar përmirësimet në performancën seismike si punë të mundshme në të ardhmen.

***Fjalët kyçe:** Muraturë e papërforcuar, Analiza statike jolineare, modelim me metodën e elementeve të fundm, veprimet sismike, metoda përforcimi.*

ACKNOWLEDGEMENTS

First and foremost, I extend my sincere appreciation to my thesis supervisor, Assoc. Prof. Mirjam Ndini, for her unwavering support, guidance, and valuable insights throughout the research process.

Special thanks are due to Assoc. Prof. Altin Bidaj and Dr. Marjo Hysenliu, who provided technical assistance and expertise in data analysis, laboratory work. Their collaboration enhanced the robustness of the methodology and results.

I am grateful to my friends and family for their encouragement and understanding during the demanding phases of thesis preparation. Their emotional support provided the necessary strength to persevere through challenges.

TABLE OF CONTENTS

ABSTRACT	iv
ABSTRAKT.....	vi
ACKNOWLEDGEMENTS	viii
LIST OF TABLES	xii
LIST OF FIGURES	xiv
LIST OF ABBREVIATIONS	xvii
CHAPTER 1	1
INTRODUCTION	1
General	1
Objective of thesis.....	2
Scope of work and methodology	2
Organization of the thesis.....	3
CHAPTER 2	4
LITERATURE REVIEW.....	4
2.1 Earthquake design codes	4
2.1.1 KTP-N.2- 89 Design Codes.....	5
2.1.2 Eurocode 6 and 8.....	7
2.2 Albanian Territory Seismicity.....	13
2.3 Failure mechanisms.....	15
2.3.1 Performance of URM walls.....	15
2.3.4 Basic failure mechanism of masonry walls	17

2.4 Material properties	18
2.4.1 Characteristics of Bricks and Mortar.....	18
2.4.2 Masonry properties.....	19
2.4.3 Compressive strength f_k	19
2.4.4 Stress-strain (σ - ϵ) relationship	20
2.5 Strengthening techniques used in existing URM structures	21
CHAPTER 3	22
ASSESSMENT OF THE CASE STUDY BUILDING	22
3.1 Introduction.....	22
3.2 Historical Investigations of this Case Study	22
3.3 Description of the Unreinforced Masonry Building	23
3.4 Seismic Conditions of the site.....	27
CHAPTER 4	29
ANALYTICAL MODELLING AND ASSESSMENT	29
4.1 Non-linear Modeling of Masonry Buildings.....	29
4.2 Modelling strategies	29
4.2.1 Tremuri Modeling Methodology.....	30
4.2.2 Modal Analysis of the Structure.....	30
4.2.3 Pushover Analysis	31
4.2.4 The N2 Method	32
CHAPTER 5	34
LABORATORY TESTS.....	34
5.1 Laboratory testing and results	34

5.3 Calculation of the Material Characteristics for the Case Study building.....	36
CHAPTER 6	38
RESULTS AND DISCUSSIONS	38
6.1 Modal Analysis Outputs.....	38
6.2 Procedure of non-linear pushover analysis	38
6.3 Conclusions	47
CHAPTER 7	49
METHODOLOGY AND PROPOSED STRENGTHENING OF EXISTING STRUCTURE	49
7.1 General Overview	49
7.2 Methodology for Repair and Strengthening of Structural Elements.....	50
7.3 Strengthening of Structural Elements	54
CHAPTER 8	59
OUTPUTS OF THE ANALYSES OF THE REINFORCED OBJECT	59
CHAPTER 9	62
CONCLUSIONS.....	62
9.1 Conclusions	62
9.2 Comparison of Structural Capacity Before and After Reinforcement.....	62
9.3 Recommendations for future research.....	64
REFERENCES.....	65
APPENDICES	67

LIST OF TABLES

Table 1. Resistance of masonry in MPa depending on the mortar strength and the type of bricks according to the Albanian design codes (KTP-N.2-89).....	5
Table 2. Value of structural coefficient.....	6
Table 3. Values of Dynamic Coefficient β_i	6
Table 4. Value of importance factor K_r	6
Table 5. Value of seismic coefficient K_E	6
Table 6. Value of k factor [EN 1996-1, 2005].....	7
Table 7. f_{vk} of Masonry.....	8
Table 8. Ground categories.....	9
Table 9. Parameters related to ground types(A-E).....	10
Table 10. Behaviour factor.....	10
Table 11. Earthquakes in the 19 th and 20 th centuries.	14
Table 12. a_g of a return period of 475 years.....	28
Table 13. a_g of a return period of 95 years.....	28
Table 14. Data from compression tests on floor slabs.	34
Table 15. Compression Test Results for Concrete Blocks.....	35
Table 16. Compression Test Results for Clay Bricks on the Third Floor.....	35
Table 17. Compression Test Results for Mortar.....	36
Table 18. Details regarding bricks and masonry characteristics taking by blueprints.....	36

Table 19. Masonry Properties	36
Table 20. Calculated parameters from the projected building characteristics	37
Table 21. The fundamental data from the modal analysis of the structure	38
Table 22. Pushover analysis parameters of building.....	46
Table 23. Global displacement drift capacities (%).....	46
Table 23. Global displacement drift capacities (%).....	46
Table 24. Comparison of global mechanical characteristics of the building before and after reinforcement	63

LIST OF FIGURES

Figure 1: Ground Type A-E (Elastic response spectra of Type 1)	10
Figure 2. Demand spectra adjusted to 1.0g p.g.a. for continuous ductilities on the Sa-Sd format.....	12
Figure 3.Capacity curve and structural performance levels.....	13
Figure 5. Failure Type(Out of plane)(D'Ayala and Speranza 2003).....	16
Figure 4. Failure modes of in-plane loaded URM walls: (a) shear failure; (b) sliding failure; (c) rocking failure; and (d) toe crushing failure(Mustafaraj 2016).	16
Figure 6. Compression Failure of Masonry	17
Figure 7. Shear Failure.....	17
Figure 8. Flexural bending failure.....	18
Figure 9. σ - ϵ diagram used to find Modulus of Elasticity(Hysenlliu 2021)	20
Figure 10. The inspected object on the field	23
Figure 11. The floor plan of the basement level.	24
Figure 12. The floor plan of the first floor.	24
Figure 13. The floor plan of the second floor.	24
Figure 14. Observation of the masonry on the ground floor where concrete blocks are visible.	25
Figure 15. Damage to perimeter walls on the top and ground floor.	26
Figure 16. Separation of load-bearing structural elements from non-load-bearing walls.	26

Figure 17. Areas of the structure that are more vulnerable to the phenomenon of structural torsion during seismic vibrations.	27
Figure 18. Elastic spectra for both horizontal and vertical response at both performance levels according to EC8 for the structure	28
Figure 19. Modelling Strategies: Macromodelling (a), Micromodelling (b), Mesomodelling (c)	29
Figure 20. MDOF to SDOF	33
Figure 21. Curve Bi-linearization	33
Figure 22. Pushover analysis cases	39
Figure 23. Load patterns and different cases of pushover analysis.....	40
Figure 24. x and y worst case scenario	40
Figure 25. Pushover analysis for x-dir, 12 load patterns of case-study building	41
Figure 26. Pushover analysis for Y-dir, 12 load patterns of case-study building	41
Figure 27. Capacity curve in x and y-direction, worst scenario.....	42
Figure 28. Normalized bilinear capacity curve in x-direction	42
Figure 29. Normalized bilinear capacity curve in y-direction	43
Figure 30. Most Damaged sections of the object.....	44
Figure 31. Failure mechanism.....	45
Figure 32. 3d view	46
Figure 33. Capacity Curve vs. Demand Spectrum for the unreinforced object	47
Figure 34. Different methodologies for the implementation of concrete jacketing in the structure.....	51

Figure 35. The cleaning and repair of existing surface cracks on the floor slab.....	52
Figure 36. The application of primer according to the manufacturer's specifications,	53
Figure 37. The placement of carbon fibers.	53
Figure 38. The details of foundation reinforcement.....	54
Figure 39. The details of column installation in the perimeter wall.	55
Figure 40. Reinforced plan of the three-story structures.....	56
Figure 41. Reinforcement of the perimeter wall with steel mesh.	57
Figure 42. Reinforced plan of structures with carbon fibers CFRP.....	58
Figure 43. Close view of the column Insertion.....	59
Figure 44. x and y-direction worst case scenario for the reinforced object	60
Figure 45. Capacity curve in x and y-direction, worst scenario.....	60
Figure 46. Normalized bilinear capacity curve in x-direction	61
Figure 47. Normalized bilinear capacity curve in y-direction	61
Figure 48. Comparison of structure capacity with earthquake spectrum.....	62
Figure 49. Comparison of capacity curves in the X direction.....	63
Figure 50. Comparison of capacity curves in the Y direction.....	64

LIST OF ABBREVIATIONS

URM	Unreinforced masonry building
$[E]$	Masonry modulus of elasticity KTP
$[Q_k]$	Weight of building KTP
$[\beta]$	Dynamic coefficient KTP
$[k_c]$	Seismic coefficient KTP
$[T]$	Period of structure
$[f_b]$	Brick compressive strength EC6
$[K_r]$	Importance factor KTP
$[f_m]$	Mortar compressive strength EC6
$[f_k]$	Compressive strength of masonry EC6
$[f_t]$	Tensile strength of masonry EC6
$[f_{vk}]$	Shear strength of masonry EC6
$[f_{vk0}]$	Initial shear strength of masonry EC6
$[G]$	Shear modulus of masonry
$[q]$	Behaviour factor EC8
$[S]$	Soil factor EC8
$[T_B, T_C, T_D]$	Characteristic periods of response spectrum EC8
$[ag]$	Ground acceleration
$[P. G. A.]$	Peak ground acceleration

$[\varepsilon_{ult}]$	Ultimate strain
$[E_b]$	Brick modulus of elasticity
$[\sigma - \varepsilon]$	Stress-strain relationship
K	Empirical coefficient depending on masonry classification EC6
$[f_{xk1}]$	Flexural strength with a plane of failure parallel to the bed joints
$[f_{xk2}]$	Flexural strength with a plane of failure perpendicular to the bed joints
$[\sigma - \varepsilon]$	Stress-strain relationship
$[d_y]$	Yield displacement of structure N2 method
$[U]$	Displacement vector N2-method
$[R]$	Inertial force vector N2-method
$[a]$	The ground acceleration as a function of time N2-method
$[P]$	Statically applied external loads N2-method
$[m^*]$	Equivalent mass of SDOF system N2-method
$[d^*]$	Displacement of equivalent SDOF system N2-method
$[F^*]$	Force of equivalent SDOF system N2-method
$[V]$	Base shear force of MDOF system N2-method
$[T^*]$	Initial period of equivalent SDOF system N2-method
$[K^*]$	Elastic stiffness of equivalent SDOF system N2-method
$[d_y^*]$	Yield displacement of bilinear capacity curve N2-method

$[K^*]$	Elastic stiffness of equivalent SDOF system N2-method
$[E_m^*]$	Energy of dissipation of equivalent SDOF system N2-method
$[\mu]$	Ductility factor N2-method
DL	Damage Limitation state EC-8
SD	Significant damage state EC-8
NC	Near Collapse state EC-8

CHAPTER 1

INTRODUCTION

General

The recent powerful earthquakes in Albania have starkly revealed the insufficient seismic resilience of the current inventory of buildings. Albania, situated at the intersection of the Eurasian and African tectonic plates, experiences seismic activity that poses a significant risk to its built environment. A powerful earthquake struck the central-western region of Albania on November 26, 2019. It was given a Mw 6.4 rating. The epicenter of the earthquake was situated offshore in the northwest of Durrës, approximately 7 km north of the city and 30 km west of Tirana, the country's capital. It had a focal depth of roughly 10 kilometers [1]. The predominant types of buildings in Albania's building stock are structures with massive load-bearing walls and buildings with reinforced concrete skeleton systems and non-load-bearing partition walls made of bricks or concrete [2]. In some cases, mixed systems are also observed. The majority of current buildings have been constructed based on the Albanian seismic code, which were first implemented as legal provisions in 1963 and have been improved and updated in 1978 and 1989. Many structures, including those from the 1940s, were designed and constructed before the advent of modern seismic design codes, raising questions about their structural integrity under seismic loading. Taking into account earlier seismic codes (such as KTP-63, KTP-2-78, KTP-N.2-89) where seismic loads were either not considered or were considered very low during the design process, this has resulted in a deficiency. To address this deficiency, there is a growing need for seismic assessment and retrofitting of existing buildings to bring them up to modern seismic safety standards. Retrofitting measures can include strengthening structural elements, adding bracing systems, and improving the overall seismic performance of the building [9]. These efforts are crucial for reducing the risk of damage during seismic events and also necessary for preserving cultural heritage. One notable category of structures in Albania comprises those constructed in the 1940s, characterized by their load-bearing concrete block walls. These buildings, representative of their time, have contributed significantly to the country's urban fabric, offering both historical and architectural value.

This paper aims to investigate the behavior of load-bearing concrete block structures from the 1940s in Albania when subjected to seismic forces. In addition to analyzing the existing structural vulnerabilities, this study addresses the critical aspect of retrofitting. Despite the scarcity of literature on load-bearing masonry structures as a traditional building technique, the inspection conducted on site, along with the expertise group, has been instrumental in comprehending all the existing damages to the structure. The findings of this research will not only contribute to the understanding of the behavior of load-bearing concrete block structures combined with clay bricks but will also offer practical insights into the seismic retrofitting of historical buildings, a topic of global significance in the realm of structural engineering and heritage preservation.

Objective of thesis

The primary goal of this thesis is to evaluate the seismic performance and safety of a three-story unreinforced masonry (URM) structure constructed at a time when seismic evaluation wasn't considered during design calculations. The building was constructed in accordance with the outdated Albanian Desing Code [KTP-63]. Taking into account the nonlinear behavior of structural elements is crucial in order to get the results of the pushover analysis which are used to evaluate the structure's performance.

Future research should consider focusing on the enhancements in seismic performance through a post-intervention analysis.

Scope of work and methodology

Because it was so affordable, masonry was commonly employed in Albania throughout the communist era (1944–1990). An approach to performance-based evaluation is necessary to appraise their real circumstances. In general, analyzing existing structures calls for distinct and different techniques than analyzing new structures. Non-linear static analysis was performed utilizing the following tools:

- TREMURI
- Excel

Organization of the thesis

The organization is conducted as below:

- **Chapter 1:** Introduction provides essential information about the topic and outlines the objectives addressed in this thesis.
- **Chapter 2:** Sources introduces the references and resources that supported data collection.
- **Chapter 3:** Assessment focuses on the evaluation of the case study building.
- **Chapter 4:** Methodology outlines the research approach adopted for the study.
- **Chapter 5:** Laboratory Tests details all the conducted laboratory experiments.
- **Chapter 6:** Analysis Results presents the findings from linear modal and non-linear static analyses, including interpretations such as first modes and pushover curves for the case study buildings.
- **Chapter 7:** Methodology and Proposed Strengthening of Existing Structure delves into the proposed strengthening methods, forming a crucial part of the research.
- **Chapter 8:** Reinforced Buildings interprets the results of the reinforced case study buildings, emphasizing pushover curves.
- **Chapter 9:** Data Interpretation and Conclusion compiles results from previous chapters and involves a thorough comparison, investigation, and deduction. This chapter concludes with overall findings, research limitations, and recommendations for future studies.

CHAPTER 2

LITERATURE REVIEW

Understanding the displacement capability under seismic forces of a unreinforced masonry object is given particular attention in this chapter. In order to analyze buildings' vulnerability, several writers have developed different theories and evaluation techniques. This chapter includes a comprehensive assessment of the literature covering the following important subjects:

- Construction codes
- The Albanian territory's seismicity
- Failure mechanisms of masonry wall
- The material properties of masonry structures and the methods used to ascertain them
- Response Spectrum

2.1 Earthquake design codes

Since Albania is a European country gradually bringing itself into compliance with EU norms, the European Codes (EC) are mandatory laws when it comes to building. To find any possible code flaws, it is imperative to compare these codes with the Albanian KTP (Kushti Teknik i Projektimit). Two notable European standards are EC-6, which deals with guidelines and regulations for masonry buildings, and EC-8, which describes the requirements for seismic design in structures.

The first building code issued in Albania at the time was KTP-1952, which established basic guidelines for construction. However, it had significant flaws, particularly in seismic analysis because seismic factors were poorly understood and building methods mostly depended on streamlined computations and prior knowledge [KTP-52, 1952]. Consequently, KTP-1963 [KTP-63, 1963] was established as the primary source of reference for building rules in 1963. This ordinance has a sizable section on masonry, which was indicative of the widely used building methods of the time.

The principal regulation governing masonry constructions that included seismic calculations was KTP-N.2-78. After the disastrous 1979 earthquake in Shkodra, which severely damaged many masonry structures erected under KTP-63, revisions were made, but the seismic requirements in KTP-89 and other later codes remained unchanged. The seismic demand in Albanian Design Codes, when compared with EN 1998-1 is observed to be lower.

2.1.1 KTP-N.2- 89 Design Codes

The design criteria of KTP-N.2-89, provide the minimum allowable values for the physical and materials' mechanical characteristics to be used. As shown in Table 1, the class of mortar and clay brick result in having a value of compression strength of a wall.

Table 1. Resistance of masonry in MPa depending on the mortar strength and the type of bricks according to the Albanian design codes (KTP-N.2-89).

Clay brick class (kg/cm ²)	Mortar class kg/cm ²						
	100	75	50	25	15	4	0
150	22	20	18	15	13.5	12	8
100	18	17	15	13	11	9	6
75	15	14	13	11	9	7	5
50	-	11	10	9	7.5	6	3.5

The formula for seismic force is conducted as below:

$$E_{ki} = K_E * K_r * \psi * \beta_i * \eta_{ki} * Q_k \quad (1)$$

Q_k is considered as a vertical force (summation of 0.9 W+0.4 short duration load + 0.8 long duration load).

$$\eta = 0.3 + \frac{0.6}{\sqrt{n}}, \text{ interim load} \quad (2)$$

$$\eta_{ki} = \frac{3k}{2n+1}, \text{ coefficient floor distribution} \quad (3)$$

Ψ is considered coefficient for elasto-plastic work as well as β_i is known as dynamic coefficient

K_E is referred as seismic coefficient

K_r is considered importance factor

n referred to number of floors

$$T = C_t H^{\frac{3}{4}}, \text{Vibration' Period} \quad (4)$$

$$\text{Another parameter is: } \beta_i = 0.8/T \quad (5)$$

The Equation 6 consideres spectral acceleration as shown below:

$$S_a = K_E * K_r * \psi * \beta_i * g \quad (6)$$

Table 2. Value of structural coefficient

Structural coefficient ψ
0.45-for building with unreinforced masonry walls
0.38- for Builing of reinfoeced masonry walls

Table 3. Values of Dynamic Coefficient β_i

Soil I $\beta_i=0.7/T$	Soil II $\beta_i=0.8/T$	Soil III $\beta_i=1.1/T$
$0.65 < \beta_i < 2.3$	$0.65 < \beta_i < 2$	$0.65 < \beta_i < 1.7$

Table 4. Value of importance factor K_r

Description of building	Importance factor
Extraordinary importance	1.5 - 4
Special importance	1.2 - 1.5
Normal importance	1
Secondary importance	0.5
Temporary	0

Table 5. Value of seismic coefficient K_E

Soil' Category	Seismic intensity		
	VII	VIII	IX
I	0.08	0.16	0.27
II	0.11	0.22	0.36
III	0.14	0.26	0.42

2.1.2 Eurocode 6 and 8

The presence of deficiencies in the Albanian design codes has led to understanding more of EN-1996 which represents the basic code for masonry structures[3].

The general formula to calculate the compressive strength of unreinforced masonry as shown in the Equation 7 is crucial in order to obtain the material parameters.

$$f_k = k * f_b^{0.65} * f_m^{0.25} \quad (7)$$

f_b and f_m are referred as brick and mortar strength

Table 6. Value of k factor [EN 1996-1, 2005]

Type of brick	Solid Bricks k=0.6	Rectangular vertical holes k=0.55	Circular vertical holes k=0.5
More than 1 brick width	k=0.5	k=0.45	k=0.4

Shear strength of masonry is an important parameter which is depended on the mortar type as shown in Table 7. The formula in order to calculate this parameter is shown below:

$$f_{vk} = f_{vk0} + 0.4 * \sigma_d \quad (8)$$

f_{vk0} is referred to mortar-brick cohesion

σ_d represents vertical stress

Table 7. f_{vk} of Masonry

Mortar(Masonry type-Solid Clay Bricks)	f_{vk0}	f_{vk} (lower limit)
M10 - M20	0.3	1.7
M2.5-M9	0.2	1.5
M1-M2	0.1	1.2

The elastic modulus (E) for short-term calculations is determined as given in Equation below.

$$E = 1000 * f_k \quad (9)$$

However, during the structural analysis in the serviceability limit state, E is taken as $600 * f_k$. The shear modulus (G) is considered to be 40% of the elastic modulus (E).

The permissible construction inclination is restricted to
$$v = \frac{1}{100 * \sqrt{h_{tot}}} \quad (10)$$

h_{tot} is referred to the total height of the building

In seismic design, EN-1998 provides general guidelines for structures, although it doesn't delve into masonry seismic design extensively. It offers recommendations, such as adhering to compressive strength limits. The minimum masonry compressive strength is specified as follows:

- Vertical (normal to bed face): $f_{(b,min)} = 5 \text{ MPa}$
- Horizontal (parallel to bed face): $f_{(b,min)} = 2 \text{ MPa}$

Seismic loading is influenced by ground acceleration and soil type. The soil classification is based on both ground acceleration and soil type.

The underlying ground conditions has a high influence on the earthquake vibration at the surface and correspondingly the ground characteristics very much influence the seismic response of structures[4]. The importance of such influence is taken in consideration in EN 1998-1 that requires that appropriate investigations (in situ or in

the laboratory) must be carried out in order to identify the ground conditions. Guidance for such investigation is given in EN 1998-5.

Three parameters are used in the classification provided in Table 8 (reproduced from EN 1998-1) for a quantitative definition of the soil profile:

the value of the average shear wave velocity, $v_{s,30}$

the number of blows in the standard penetration test (NSPT)

the undrained cohesive resistance C_u

Table 8. Ground categories

Ground type	Description	Parameters		
		$v_{s,30}$ (m/s)	NSPT (blow/30cm)	C_u (kPa)
A	Rock or other rock like geological formation, including at most 5m of weaker material of the surface	>800	-	-
B	Deposits of very dense sand, gravel, or very stiff clay, at least several tens of meters in thickness, characterised by a gradual increase of mechanical properties with depth.	360-800	>50	>250
C	Deep deposits of dense or medium dense sand, gravel or stiff clay with thickness from several tens of hundreds of meters.	180-360	15-50	70-250
D	Deposits of loose to medium cohesion-less soil (with or without some soft), or of predominantly soft to firm cohesive soil	<180	<15	<70
E	A soil profile consisting of a surface alluvium layer with v_s values of type C or D and thickness varying between about 5m and 20m, underlain by stiffer material with $v_s > 800$ m/s			
S1	Deposits consisting, or containing a layer at least 10 m thick, of soft clays/silts with a high plasticity index ($PI > 40$) and high water content	<100	-	10-20
S2	Deposits of liquefiable soils, of sensitive clays, or any other soil profile not included in types A-E or S1			

Response spectrum represents the seismic activity.

According to EN 1998-1, there are two different kinds of reaction spectrums based on magnitude:

When predicted magnitudes of $M > 5.5$, type 1 is employed which represents high seismicity

Type 2: utilized when anticipated magnitudes M less than 5.5

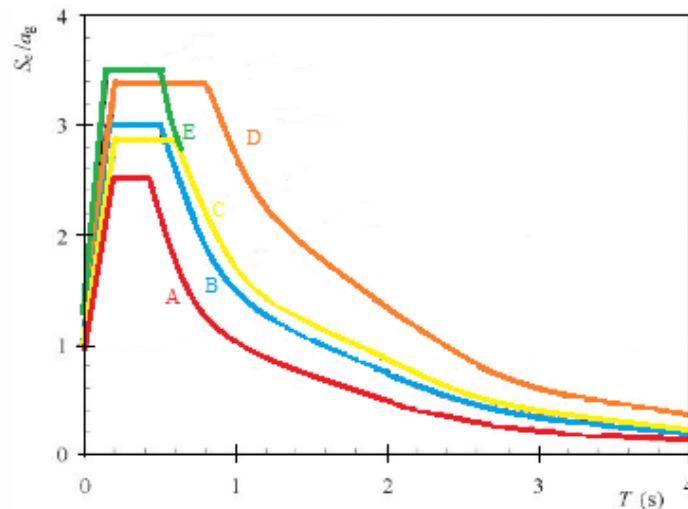


Figure 1: Ground Type A-E (Elastic response spectra of Type 1) [4]

In order to get the proper elastic spectral response $S_e(T)$ is needed to be known the Soil Type and characteristics period T_B , T_C , $T_D(s)$ as shown in Table 9 and Table 10.

Table 9. Parameters related to ground types(A-E)

Soil type	A	B	C	D	E
S	1.0	1.2	1.15	1.35	1.4
T_B(s)	0.15	0.15	0.2	0.2	0.15
T_C(s)	0.4	0.5	0.6	0.8	0.5
T_D(s)	2.0	2.0	2.0	2.0	2.0

Table 10. Behaviour factor

Type of construction	q
Unreinforced masonry in accordance with EN 1996 alone (recommended only for low seismicity cases)	1.5
Unreinforced masonry in accordance with EN 1998-1	1.5 - 2.5
Confined masonry	2.0 - 3.0
Reinforced masonry	2.5 - 3.0

The relationships that follow are used to compute peak ground acceleration in the design response spectrum:

For periods $0 \leq T \leq T_B$, the seismic design acceleration $S_D(T)$ is calculated using the Equation 11.

$$a_g * S * \left[\frac{2}{3} + \frac{T}{T_B} \left(\frac{2.5}{q} - \frac{2}{3} \right) \right] \quad (11)$$

For periods $T_B \leq T \leq T_C$, the formula becomes $a_g * S * \frac{2.5}{q}$ (12)

Moving on to periods $T_C \leq T \leq T_D$, the equation is more complex: $S_D(T)$ takes the value $\left\{ \begin{array}{l} a_g * S * \frac{2.5}{q} * \frac{T_C}{T} \\ \geq \beta * a_g \end{array} \right\}$ (13)

and for $T \geq \beta * a_g$, it becomes $\left\{ \begin{array}{l} a_g * S * \frac{2.5}{q} * \frac{T_C * T_D}{T^2} \\ \geq \beta * a_g \end{array} \right\}$ (14)

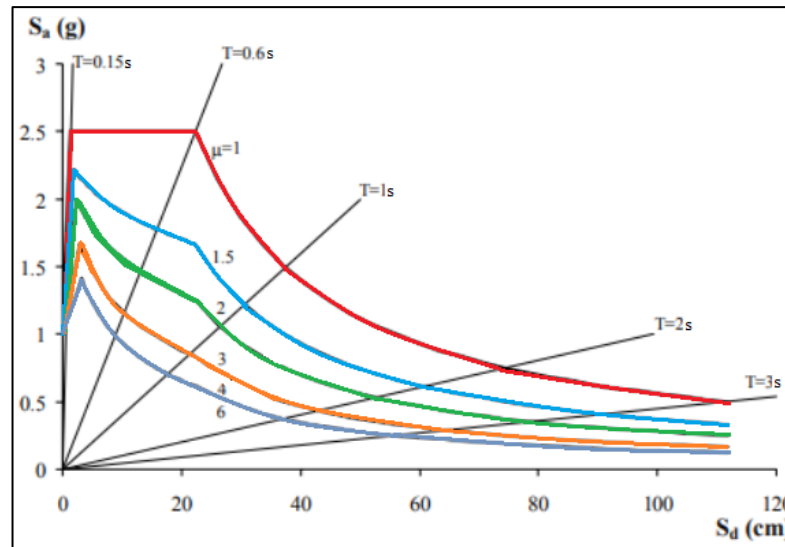


Figure 2. Demand spectra adjusted to 1.0g p.g.a. for continuous ductilities on the S_a - S_d format.

The above spectrum (elastic) is converted to inelastic according to the EC-8 procedure, and in the end, it is presented as a function of spectral acceleration and spectral displacement. This approach is taken so that, in the end, the capacity of the structure can be compared with the spectrum, leading to conclusions about the performance and condition of the structure in the event of a specific earthquake.

By definition, the capacity of the structure is the maximum level of horizontal force that it can withstand without collapsing (this when the building is loaded with gravity loads). According to EC-8, the structural capacity of the building is assessed through nonlinear pushover analysis and is presented in terms of the force-displacement graph of the idealized model with a structural freedom scale. For ease of calculation, the capacity curve is taken as bi-linear, clearly distinguishing the initial elastic and plastic phases.

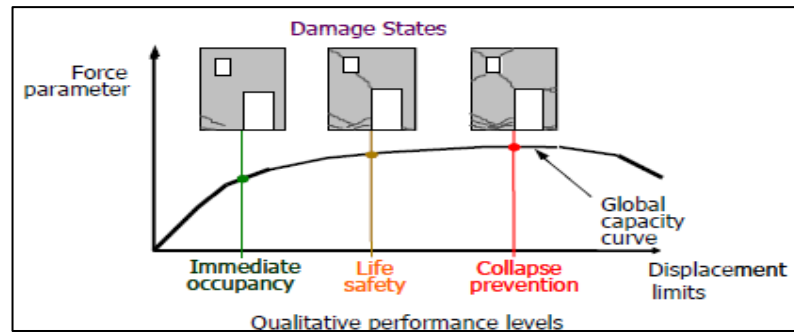


Figure 3. Capacity curve and structural performance levels[15]

By the structural performance level, we refer to the expected extent of damage that the structure may have after a specific earthquake. EC-8 classifies 3 performance levels as follows:

- **DL Damage Limitation:** In this phase, there are no structural damages to the building, but there may be damages to non-structural elements. Most elements operate in the elastic phase, and the structure is ready to continue its functionality.
- **SD Significant Damage:** In this phase, there are structural damages, but they are repairable and do not threaten the lives of residents. Most elements have exceeded the elastic phase, and some may reach their plastic capacity (develop various cracks). The structure needs reconstruction before resuming its functionality.
- **NC Near Collapse:** In this phase, there are severe structural damages, and the lives of residents may be at risk. Most elements operate in the plastic phase, and there may be local collapses. At this stage, the building is likely to be uneconomical to repair, as the cost of repair approaches values comparable to reconstruction.

2.2 Albanian Territory Seismicity

Albania has a moderate degree of seismic danger due to its location on the Alpine-Mediterranean seismic plate. High-intensity earthquakes have occurred in the area in the past. Frequent episodes of intense seismic micro-activity, usually with magnitudes between $1.0 < M < 3.0$, are what define Albania's seismicity. There are also a lot of minor earthquakes with magnitudes between 3.0 and 5.0. Strong earthquakes ($M > 7.0$)

are extremely unusual events, whereas medium-sized earthquakes ($5.0 < M < 7.0$) are uncommon[5].

Significant earthquakes have occurred in Albania, most notably in the northwest near Shkodra. For example, the earthquake that occurred on June 1, 1905, had a magnitude of $M_s = 6.6$, lasted for 10–12 seconds, and resulted in significant damage. On April 15, 1979, a large earthquake with a magnitude of 6.6 to 7.2 struck close to Petrovac, Montenegro [Sulstarova et al., 2005]. The zonation map and seismic code were updated in response to this earthquake event. On November 26, 2019, Durres was affected by a powerful earthquake with a magnitude of 6.4. There were many deaths as a result of its epicenter being perilously near to thickly inhabited regions[6]. Historic masonry structures in Tirana's Thumane, Vore, and Kombinat neighborhoods sustained significant damage, with some of the buildings toppling.

Table 11. Earthquakes in the 19th and 20th centuries.

<i>City</i>	<i>Year of occurrence</i>	<i>Intensity</i>	<i>Casualties</i>
	1855		Io>VIII, destroyed 3 villages
	1905		1500 houses destroyed completely
Shkoder	1948	Magnitude 6.6	N.A
	1979		17122 buildings were almost destroyed, affected Lezha, too.
Leskovik	1919		N.A
Tepelene	1920		250 housed destroyed or heavily damaged
	1969		N.A
Elbasan	1920		173 houses destroyed completely
	1931		N.A
Diber	1942		495 houses destroyed completely, 929 buildings were heavily damaged, 2200 were affected
	1967		534 houses destroyed, 1623 heavily damaged
Durres	1926		most of the houses destroyed, the portal of the city castle was demolished
	1833		N.A
	1851		Io=IX, 2000 killed
Vlore	1859	Magnitude 6.6	N.A
	1866		N.A
	1930		almost destroyed 3 villages, 494 houses

	1963		N.A
Librazhd	1935		N.A
	1967		N.A
Lushnje	1959		761 houses collapsed
	1982		N.A
Korce	1960		103 houses collapsed, 878 were heavily damaged
	1962		about 1000 houses were destroyed or heavily damaged
	1969	Magnitude 6.6	Io=VIII destroyed or heavily damaged 842 buildings, affecting cities nearby too.
Fier	1982		278 houses collapsed, 2186 were heavily damaged, affected the cities of Lushnje and Berat
Tirane	1988	Magnitude 5.4	, Io=VII, PGA=0,4048g

2.3 Failure mechanisms

2.3.1 Performance of URM walls

The analysis of masonry structures is a rather complex task due to the particular nature and the mechanical behavior of masonry due to the lack of homogeneity and standardization. Understanding the mechanical behavior of URM buildings is one of the most complex and challenging issues of structural engineering. When analyzing masonry, a prominent feature to be considered is the softening behavior, which is typical of quasi-brittle materials. Softening is a gradual decrease of mechanical resistance under a continuous increase of deformation, caused by progressive internal crack growth, generally attributed to the heterogeneity of the material, due to the presence of different phases and material defects, like flaws and voids[7].

Usually, the bond between brick unit and mortar is considered to be the weakest link in masonry assemblage. The nonlinear response of the mortar joints is associated with two types of failure modes: tensile failure (mode I) and shear failure (mode II) [12].

2.3.2 Out-of-Plane Failure

Out-of-plane failure in masonry refers to the collapse or tilting of a wall or structure perpendicular to its intended plane. This failure mode typically occurs when the wall

lacks sufficient lateral support or is subjected to excessive horizontal loads, such as those generated during seismic events. The masonry units or mortar joints may fail, leading to sudden collapse or out-of-plane displacement. This failure mode poses a significant risk to the overall stability of the structure.

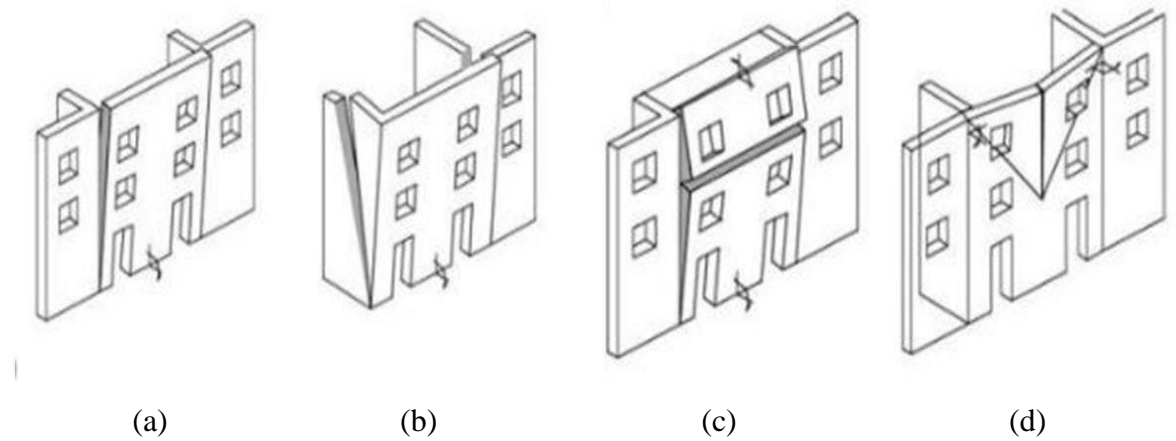


Figure 4. Failure Type(Out of plane)[8]

2.3.3 In-Plane Failure

In-plane failure, on the other hand, involves failure mechanisms occurring within the intended plane of the masonry structure. Common in-plane failure modes include compression failure, shear failure, flexural failure, and tensile failure. These mechanisms manifest as cracks, deformations, or local damage within the plane of the wall or structure. In-plane failure often results from applied vertical or lateral loads that exceed the masonry's capacity to resist them. Retrofitting and strengthening measures are implemented to enhance the in-plane performance of masonry structures, particularly under seismic or other dynamic loads.

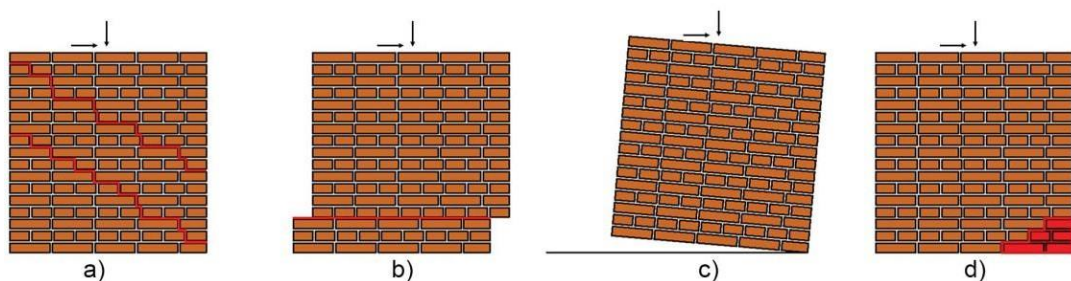


Figure 5. Failure modes of in-plane loaded URM walls: (a) shear failure; (b) sliding failure; (c) rocking failure; and (d) toe crushing failure[9].

2.3.4 Basic failure mechanism of masonry walls

Compression Failure: This occurs when the masonry material is unable to withstand the compressive forces acting on it. It often leads to the crushing or buckling of the masonry elements.

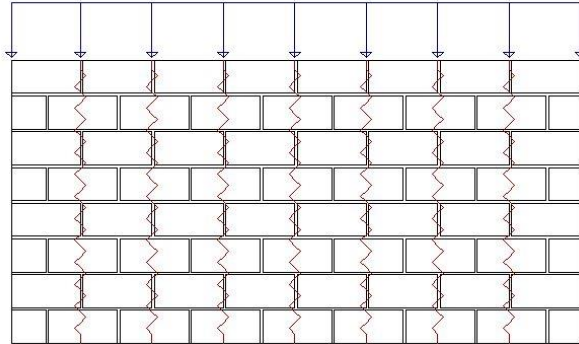


Figure 6. *Compression Failure of Masonry*[23]

Shear failure happens when the applied forces cause the individual layers or units of masonry to slide or deform relative to each other. It can result in diagonal cracking or sliding along mortar joints.

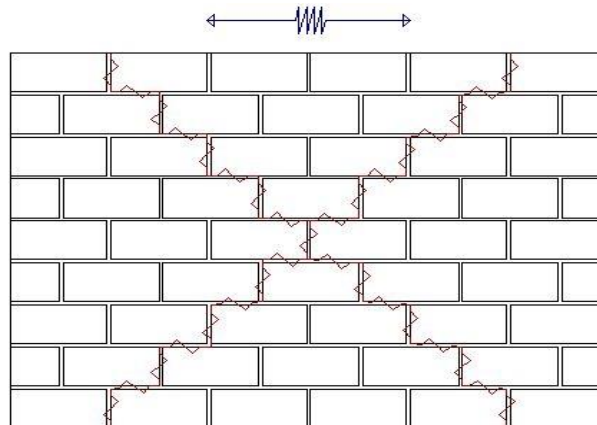


Figure 7. *Shear Failure*

Flexural failure involves the bending or cracking of masonry elements due to applied loads. It often occurs in response to lateral forces or moments, leading to cracks and damage.

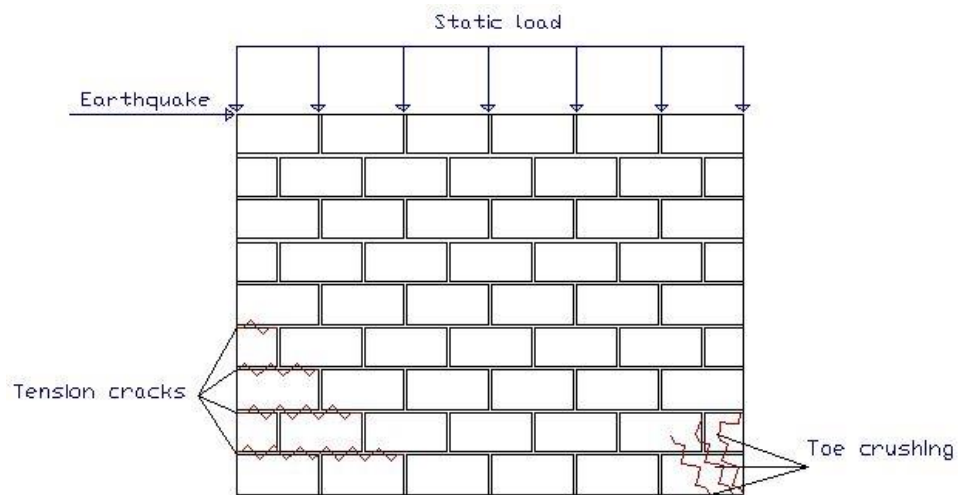


Figure 8. *Flexural bending failure*

Masonry is generally weak in tension. Tensile failure occurs when the masonry material is subjected to pulling or stretching forces, leading to cracking and separation of the material.

2.4 Material properties

The qualities of the constituent materials and their interactions give masonry its attributes as a composite construction material. These components consist of reinforcing steel, concrete infill, bonding materials, and masonry units. Masonry is divided into three subgroups: unreinforced, confined, and reinforced, depending on how these components are put together inside a structure.

Understanding the behavior of a URM structure is crucial for determining its properties, such as brick compressive strength, Modulus of Elasticity, and stress-strain behavior.

2.4.1 Characteristics of Bricks and Mortar

More often, silicate and clay brick masonry are utilized in a variety of buildings. Bricks considered strong in compression but weak in tension because of their high porosity and brittleness. Two categories are known (silicate and clay bricks). First one are represented by two grades (M7.5 and M10) as well as clay bricks by (M5 and M7.5)[10].

2.4.2 Masonry properties

The combined mechanical properties play a crucial role in determining bearing capacity of walls and structures when subjected to both vertical and lateral loads. However, as demonstrated earlier, these masonry properties are inherently influenced by material characteristics. The fundamental qualities outlined in EC-6 [3] are essential, and it is recommended to obtain them through standardized testing procedures as outlined in EN1052.

- Compressive strength (f_k): The resistance of masonry to being crushed.
- Shear strength (f_v): The ability of masonry to withstand lateral forces.
- Flexural strength (f_x): The capacity of masonry to resist bending.
- Stress-strain relationship (σ - ϵ): The correlation between applied stress and resulting strain.
- Tensile strength (f_t): The masonry's ability to resist tension, equivalent to shear strength (f_v).
- Modulus of elasticity (E): The measure of masonry's stiffness.
- Shear modulus (G): The material's response to shear stress.
- Ductility factor (μ): The extent of masonry's ability to deform without failure.

These qualities are critical for assessing the overall performance and safety of masonry structures. It's advised to determine them using the recommended standard test procedures in EN1052.

2.4.3 Compressive strength f_k

Several factors affect masonry compressive strength, including craftsmanship, properties of masonry units, mortar joint thickness, mortar age, and the suction rate of bricks.

According to Eurocode 6, the relationship between brick unit, mortar, and masonry compressive strength(f_k) is expressed by the equation:

$$K * f_b^{0.7} * f_m^{0.3} \quad (15)$$

Here, f_b represents the normalized mean compressive strength of brick units, f_m is the normalized mean compressive strength of mortar, and K is an empirical coefficient dependent on masonry classification. The constants α and β have fixed values of 0.7 and 0.3, respectively, while k , α and β may vary within certain ranges.

2.4.4 Stress-strain (σ - ϵ) relationship

In the absence of experimental evidence, EC-6 advises determining the modulus(E) expressed $1000 * f_k$.

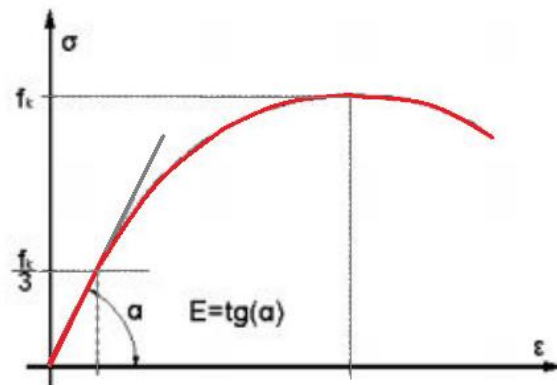


Figure 9. σ - ϵ diagram used to find Modulus of Elasticity[11]

2.4.4.1 Elastic Modulus

In the absence of experimental data, Pauley [Pauley et al., 1997] suggests a modulus of $E = 1000f_k$ [MPa], Binda [Binda, 2007] suggests $E = 900$ N/mm² for impoverished rural buildings, $E = 900$ -1500 N/mm² for civil buildings and palaces, while Tomazevic [Tomazevic, 1999] suggests $200 f_k \leq E \leq 2000f_k$.

2.4.4.2 Shear Modulus

According to EN 1996-1, 2005, the shear modulus G can be calculated as 40% of the modulus of elasticity, E . When expressing shear modulus in terms of tensile strength, $G = 2000f_t$ is the suggested value.

2.5 Strengthening techniques used in existing URM structures

Surface Handling: It is a method that hides the masonry's external face by changing the building's architectural design. It involves building a steel or polymer mesh and covering the outside of the structure with a mortar with a high strength. By confining the masonry after it has cracked, this method raises the maximum load resistance[12].

Ferrocement jacketing: A cement with mortar surface with a strength of range 15 to 30 Mpa which has a thickness of range 10 to 50mm combined with meshes which are close to each-other. It results in a significant rise in stiffness. Pre-damaged URM walls can be strengthened to regain their original stiffness and capacity. Ferrocement's excellent flexural and shear strength allow it to control the formation of cracks.

CHAPTER 3

ASSESSMENT OF THE CASE STUDY BUILDING

3.1 Introduction

Assessing an existing building's seismic performance requires a detailed review of its geometry, structural system, material properties, and load distribution. The current performance of the building has been assessed based on on-site inspection and observation of overall damages to the structure, in accordance with modern seismic codes (EC-8).

3.2 Historical Investigations of this Case Study

The building was constructed around the 1940s with a load-bearing solid wall structure made of concrete blocks without seismic reinforcements. It possesses a regular geometric plan and dimensions. The analyzed structure, building no. 14 of the AFA (serving for accommodation for the soldier of Albania), with a total area of 5062.8 m², is located within the Ministry of Defense complex on Dibra Street in Tirana. The building's structure was initially conceived as a load-bearing solid wall structure with concrete blocks, typical of Italian architecture during its construction period. However, the subsequently added third floor is also a load-bearing solid wall structure but built with clay bricks, which possess relatively lower resistance compared to concrete blocks. Its third floor was later added during the early 1990s, characterized by lower floor height and the use of different materials in its construction.

Existing conditions of the building were assessed based on a thorough on-site inspection, taking into consideration modern seismic construction codes such as EC-6 and EC-8.



Figure 10. The inspected object on the field

3.3 Description of the Unreinforced Masonry Building

A thorough visual inspection of the building involves three phases: geometry, material, and damage surveys. The three-story unreinforced masonry (URM) building, with plan dimension of 10,554 m by 1,796 m as shown in Appendix. The ground floor is 5 meters high, the first floor is 5 meters high, and the second floor is 3 meters high, each with a surface area of 1,897.6 square meters. Load-bearing walls, 0.64 m thick on the ground floor and 0.15 m thick on the first and second floors, run in both longitudinal and transverse directions.

Between the floors of the structure, there is observed a continuity of structural elements with no discontinuity issues. However, it should be noted that the last floor which was added later, while maintaining the plan form, exhibits a change in the height as well as the materials used and a significant reduction in the strength and rigidity of load-bearing walls. This is attributed to variations in the characteristics of the concrete-clay brick block. The addition of the last floor, has resulted in a reduction of the structure's capacity.

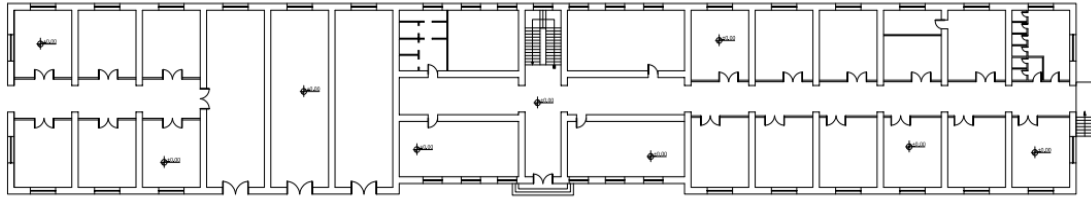


Figure 11. *The floor plan of the ground level.*

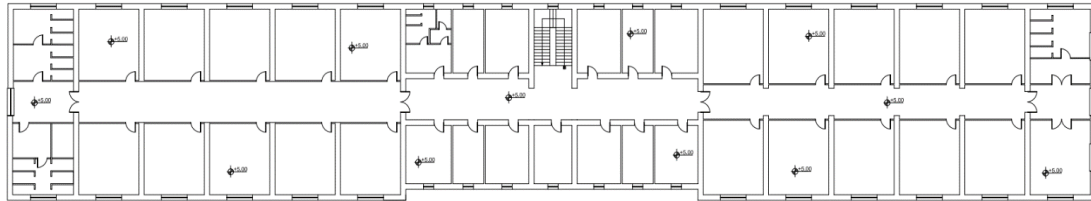


Figure 12. *The floor plan of the first floor.*

The floor slabs of the intermediate floor are monolithic with a relatively low thickness of about 0.15 m. However, they are constructed with high-strength concrete, approximately 35 MPa. To enhance the even distribution of both vertical and horizontal loads, we incorporate beams. These beams serve to establish a stronger connection between slabs and load-bearing walls.

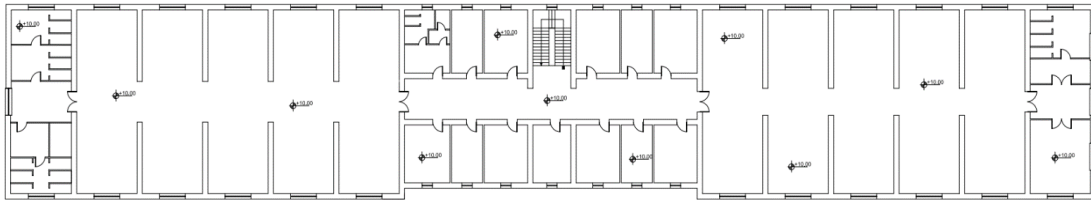


Figure 13. *The floor plan of the second floor.*

Generally, no significant damage is observed in these slabs, except for the ceiling slab of the second floor, where the presence of moisture has caused not only minor damages but also material degradation in some parts.



Figure 14. Damage to floor slabs and perimeter walls on the top floor due to the presence of moisture.



Figure 15. Division of masonry from other load-bearing elements and its loading near the joint.



Figure 14. Observation of the masonry on the ground floor where concrete blocks are visible.

Several damages are present in this building. Damages consist of cracks and small to medium sized openings. They are limited in corners, especially in the connections between the walls and between slab wall



Figure 16. Damage to perimeter walls on the top and ground floor.



Figure 15. Separation of load-bearing structural elements from non-load-bearing walls.

The longitudinal dimension is bigger than its transverse one (105.54 m compared to 17.96 m). This results in the occurrence of torsional behavior during seismic movements and causes damage in a specific part of the structure (the area where the two orthogonal elements of the building join). The solution to this problem is the use of seismic joints, which effectively divide the structure into two independent segments that move independently of each other. However, despite the presence of this seismic joint, it has been designed for two floors. Since the third floor is an addition, the two distinct parts of the structure have collided, leading to significant damage precisely in this section of the building, especially on the second floor.

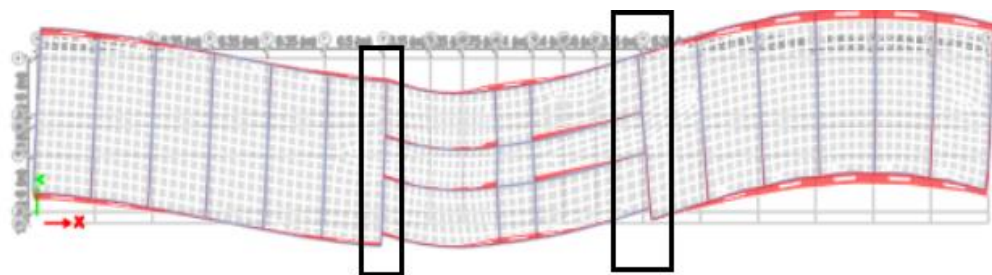


Figure 17. Areas of the structure that are more vulnerable to the phenomenon of structural torsion during seismic vibrations.

3.4 Seismic Conditions of the site

We determine the peak ground acceleration (PGA) considering soil conditions ($V_s = 450.9$ m/sec) for two different likelihood levels: a 10% chance of occurrence within 10 years and a 10% probability within 50 years. These align with two earthquake recurrence periods: 95 years and 475 years, fully adhering to Eurocode 8. The soil type is categorized as type B.

The peak ground acceleration for the 'non-collapse condition' at the foundation of this construction site has been taken from a seismologist, a value of $PGA=0.293g$. This value corresponds to a return period of 475 years (90% non-exceedance in 50 years).

Taking into account the Soil Factor for Type B, $S=1.20$, the design acceleration for the "non-collapse condition" for the upcoming work is determined as:

Table 12. ag of a return period of 475 years

Soil Factor	Max. Ground Acceleration	Desing Acceleration	Corner Periods		
			T _B	T _C	T _D
1.2	0.352	0.422g	0.15s	0.5s	2.0s

For the 90% non-exceedance level in 10 years (with a return period of 95 years), the value PGA=0.144g is determined. This assessment is based on the recommendation of the Institute of Geological, Seismological, and Environmental Studies of Albania [26] for probabilistic seismic risk assessments in the territory of Albania.

Considering the Soil Factor for Type B in this area as S=1.20, the design acceleration for the "damage limitation condition" for upcoming work is determined as:

Table 13. ag of a return period of 95 years[4]

Soil Factor	Max. Ground Acceleration	Desing Acceleration	Corner Periods		
			T _B	T _C	T _D
1.2	0.173g	0.208g	0.15s	0.5s	2.0s

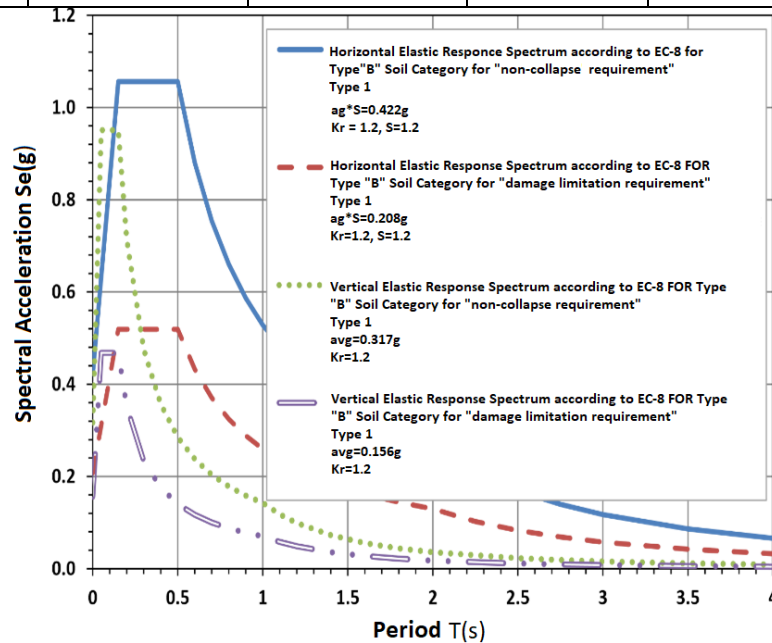


Figure 18. Elastic spectra for both horizontal and vertical response at both performance levels according to EC8 for the structure

CHAPTER 4

ANALYTICAL MODELLING AND ASSESSMENT

4.1 Non-linear Modeling of Masonry Buildings

Modeling masonry objects is challenging due to joint weaknesses, material nonlinearity, and discontinuities. An accurate model needs to consider both brick and mortar behaviors and their interaction.

4.2 Modelling strategies

MacroModelling Technique: In this technique, masonry units and mortar are modelled as a single materia in order to contain a homogeneous modelling technique[23].(Figure 22a).

MicroModelling Technique: A highly detailed form of modeling that incorporates the properties of individual units and mortar. While this model produces more precise results, it demands higher computational resources due to its increased complexity.

MesoModelling Technique: Is a more simple method of micromodelling(Figure 22c). In this technique, materials are not individually modeled but represented by equivalent elements (such as plates) with corresponding properties

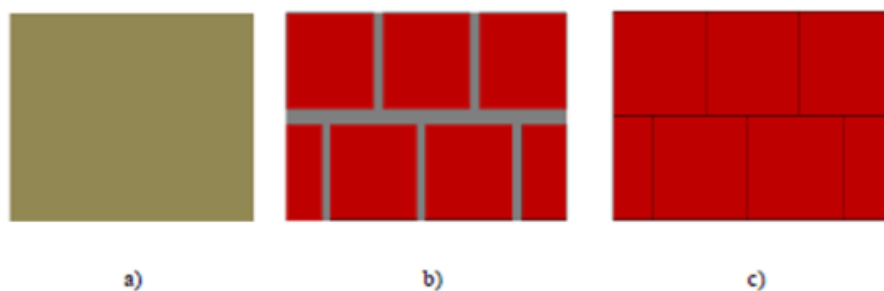


Figure 19. Modelling Strategies: Macromodelling (a), Micromodelling (b), Mesomodelling (c)

4.2.1 Tremuri Modeling Methodology

The evaluation of the TREMURI structure unfolds in two distinct phases: initially, an automated generation of the equivalent frame model transpires. Subsequently, a non-linear static analysis, commonly known as a push-over analysis, is executed to derive the structure's capacity curve, illustrating stress-displacement characteristics at the control node. The outcome of the equivalent frame model generation manifests as a visual representation, delineating the structure into components such as piers, lintels, beams, tie rods, and columns. It's noteworthy that these elements retain manual adjustability to accommodate specific scenarios. On the other hand, the non-linear analysis unfolds by progressively escalating the applied loads, yielding the horizontal displacement of the structure [19]. The determination of a predefined displacement value, automatically computed, marks the point where the structure is deemed collapsed. At this juncture, the Horizontal Force - Horizontal Displacement curve materializes, encapsulating the offered capacity curve. Essentially, this curve illuminates the structure's behavior amidst varying horizontal loads.

4.2.2 Modal Analysis of the Structure

Initially, the model has undergone modal analysis. After the structure was first subjected to modal analysis, preliminary verifications were made regarding structural regularity and the inherent vibrations of the structure. Using the computational program, the modal analysis of the structure can be easily conducted for objects with multiple degrees of freedom [20]. The basic dynamic equation for a system with multiple degrees of freedom:

$$[M]\{\ddot{U}\} + [C]\{\dot{U}\} + [K]\{U\} = -[M]\{1\}\ddot{u}_g \quad (15)$$

Where:

[M]– mass matrix

[C] – damping matrix

[F] – stiffness matrix

$\{l\}$ – displacement vector (mass) when a unit force is applied on each floor

\ddot{u}_g – ground acceleration

Taking a vector in the form of vibration modes $\{\phi\}$, which is independent of time, and assuming a relative displacement vector U , the dynamic differential equation for a system with multiple degrees of freedom can be rewritten as:

$$U = \{\phi\}u_t \quad (16)$$

Where " u_t " represents the displacement at the bottom floor, the basic dynamic differential equation can be rewritten as follows:

$$[M]\{\phi\}\ddot{u}_t + [C]\{\phi\}\dot{u}_t + [K]\{\phi\}u_t = -[M]\{l\}\ddot{u}_g \quad (17)$$

To determine the modal matrix of free vibrations $\{\phi\}$, initially, a modal analysis is conducted for the free vibrations of the structure. This is done to determine the natural frequency of free vibrations ω_i for each mode and the mode shape $\{\phi\}_i$. The equation used to calculate $\{\phi\}_i$ is:

$$([k] - \omega_i^2[m]) * \{\varphi\}_i = 0 \quad (18)$$

While for the natural frequencies of free vibrations ω_i for each mode:

$$\det|[k] - \omega_i^2[m]| = 0 \quad (19)$$

4.2.3 Pushover Analysis

The pushover analysis of a structure entails a non-linear static examination, wherein permanent vertical loads persist while lateral loads increment gradually. The equivalent static lateral loads serve as approximations for forces induced by earthquakes. Through this analysis, a plot depicting the total base shear against top displacement in the structure is generated, unveiling any premature failure or weaknesses.

This comprehensive analysis extends until failure, facilitating the determination of both the collapse load and ductility capacity. Specifically, on a building frame, the

monitoring of plastic rotation and the computation of lateral inelastic force versus displacement response for the entire structure contribute to a thorough understanding.

The significance of this type of analysis lies in its ability to pinpoint weaknesses within the structure, offering valuable insights into potential vulnerabilities that might be addressed for enhanced structural integrity.

4.2.4 The N2 Method

The N2 method, developed by Fajfar in the mid-1980s, is a non-linear seismic analysis technique for structures. The 'N' in N2 represents non-linear analysis, while '2' signifies the use of two mathematical models: a single-degree-of-freedom (SDOF) system and a multi-degree-of-freedom (MDOF) system. This method combines the pushover analysis of an MDOF model with the response spectrum analysis of an equivalent SDOF system[13].

The N2 method is formulated in the acceleration-displacement format, establishing a connection between the lateral load pattern in pushover analysis and the assumed displacement shape. This format allows for a clear interpretation of the seismic response and the relationships between key quantities. Unlike the capacity spectrum method, the N2 method employs inelastic spectra rather than elastic spectra with equivalent damping and period.

The development of the N2 method began in the mid-1980s, evolving into a more refined version over time. Recently, following Bertero's and Reinhorn's idea, the method has been further refined, presenting a transparent transformation from an MDOF to an equivalent SDOF system in the acceleration-displacement format[14].

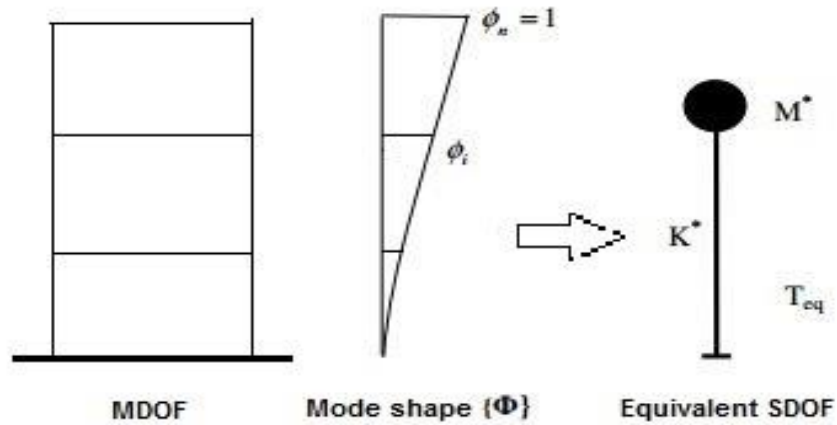


Figure 20. MDOF to SDOF [11]

In the N2 method, two mathematical models and three analysis steps are employed. In the initial step, stiffness, strength, and supplied ductility are determined through non-linear static analysis of the MDOF system under a gradually increasing lateral load. In the second step, an equivalent SDOF system is defined, assuming that the deflected shape remains constant during an earthquake. The non-linear characteristics of the equivalent system are based on the base shear vs. top displacement relationship obtained in the first step. In the third step of N2, the maximum displacement is determined through non-linear dynamic analysis of the equivalent SDOF system.

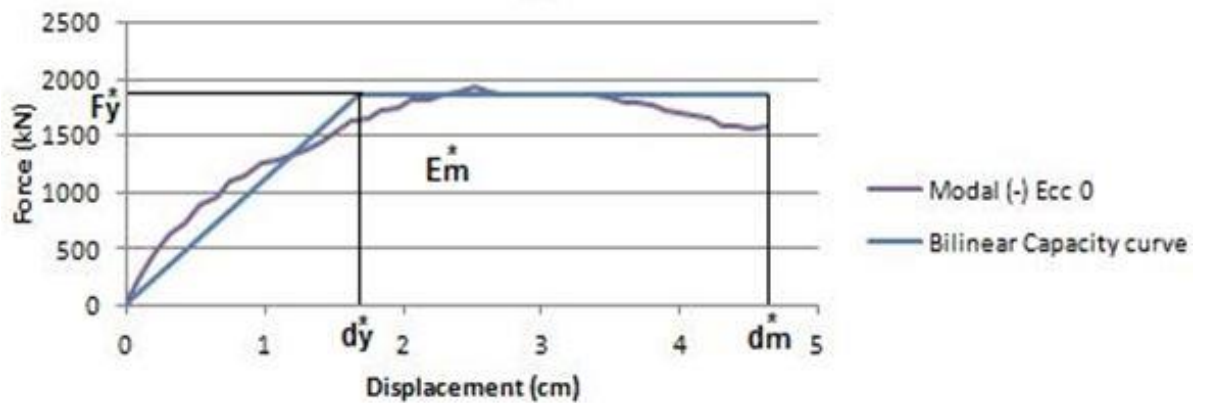


Figure 21. Curve Bi-linearization [22]

CHAPTER 5

LABORATORY TESTS

5.1 Laboratory testing and results

The information about existing materials has been derived from laboratory tests conducted on-site as part of this expertise by Altea&GeoStudio2000 and is provided alongside this assessment. Since there are no project data regarding the materials used and their physico-mechanical characteristics, their values for the utilized models and beyond will be based on these tests. It should be noted that even for the age of the building, EC recommends relying on laboratory tests for physico-mechanical characteristics.

Concerning the floor slabs, based on EN1204-1, compression tests have been performed on cores with a height/diameter ratio of 1:1, which is equivalent to cubic strength, while those with a height/diameter ratio of 2:1 are equivalent to cylindrical strength. Cores were extracted using a diamond-toothed core drill, examined in the laboratory, and compression tests were conducted after the surface was leveled with a specialized grinding device. The values for the floor slabs of each floor have been extracted from the test data as follows:

Table 14. Data from compression tests on floor slabs.

Sample	Position	Height/Diameter	Density	Compression Strength
1	First Slab	0.83	2.318 g/cm ²	35.94 MPa
2	Second Slab	0.84	2.350 g/cm ²	38.94 MPa
3	Third Slab	0.84	2.411 g/cm ²	40.15 MPa

Based on the above values, it can be concluded that the floor slabs are constructed using C30/37 concrete, which exhibits favorable strength and durability characteristics. The thickness of the floor slab is 15cm, considered acceptable given the good physico-mechanical properties of the concrete used.

Regarding the masonry, tests have been conducted for the concrete blocks for the first two floors and for the brick elements and mortar for the third floor. From the test data for the concrete blocks, it is concluded that they are made of C12/15 concrete with a strength of around 12 MPa. This value is acceptable for masonry and complies with the provisions of KTP-89 and EC-8.

Table 15. Compression Test Results for Concrete Blocks

Position	Compression Strength
First Floor	12.38 N/mm ²
Second Floor	13.22 N/mm ²

The masonry on the third floor consists of solid clay bricks with a compressive strength of $f_b=7.5$ MPa. This value is also acceptable for load-bearing masonry.

Table 16. Compression Test Results for Clay Bricks on the Third Floor

Position	Compression Strength
Third Floor	7.25 N/mm ²
Third Floor	7.81 N/mm ²

The mortar used in both cases, both in the concrete block masonry of the first two floors and in the brick masonry of the last floor, has a compressive strength of $f_m=2.5$ MPa. According to EC-8, this value is unacceptable for load-bearing structural walls, where the minimum required value is $f_m=5$ MPa. This results in poor bond between the concrete block or brick elements, reducing the tensile strength of the masonry.

Table 17. Compression Test Results for Mortar

Position	Volumetric weight	Compression Strength
1-Floor	1.311 g/cm ³	2.76 MPa
2-Floor	1.462 g/cm ³	3.25 MPa
3-Floor	1.319 g/cm ³	2.47 MPa

5.3 Calculation of the Material Characteristics for the Case Study building

The average values of material parameters obtained from laboratory tests are presented below and contribute to the implementation of numerical modeling.

Table 18. Details regarding bricks and masonry characteristics taking by blueprints

	Brick Properties		Mortar Properties	
	Type	f_b [MPa]	Type	f_m [MPa]
3 floor	Clay	7.5	Cement	2.5
1&2floor	Concrete Blocks	10	Cement	5

All the masonry properties shown below are needed for numerical modelling.

Table 19. Masonry Properties

Compressive Strength(f_k)	$K * f_b^{0.7} * f_c^{0.3}$ <p>normalized with factor $\delta(0.8)$</p> <p>Value of K is equal to 0.6</p>
Young Modulus (E)	$1000 * f_k$

CompressiveFracture Strength(G_{fc})	$15 + 0.43 * f_k - 0.0036 * f_k^2$
Tensile Strength(f_t)	$0.05 * f_k$
Shear Strength(f_{vk})	$f_{vk0} + 0.4\sigma_d$
f_{vk} max value is equal to $0.065 f_b$	f_{vk0} ranges from 0.2 in cases of clay bricks M-10 to 0.15 in cases of silicate bricks M-7.5 σ_d is equal to 1MPa
f_{xk1}	$0.035f_b$
f_{xk2}	$0.025f_b$
Shear Modulus (G)	$0.25E$
Poisson ratio (ν)	0.2

Table 20. Calculated parameters from the projected building characteristics

	f_k [MPa]	f_{vk} [MPa]	f_{vk0} [MPa]	f_t [MPa]	f_{xk1} [MPa]	f_{xk2} [MPa]	E [MPa]	G [MPa]	G_{fc} [MPa]	ν
3 floor	1.97	0.4875	0.2	0.1	0.26	0.19	1977	494	3.16	0.2
1&2floor	2.97	0.65	0.2	0.15	0.35	0.25	2970	744	4.76	0.2

CHAPTER 6

RESULTS AND DISCUSSIONS

6.1 Modal Analysis Outputs

In the following figures, 3-dimensional models have been provided for the first 6 modes of the building's vibrations. It is observed that the first and second modes of vibration exhibit a presence of torsion. This is due to the fact that, as emphasized earlier, the planimetric shape of the building has a much greater longitudinal dimension than transverse, resulting in the phenomenon of torsional motion during seismic vibrations. The diaphragm exists on the first two floors; however, it has not been respected during the addition of the third floor, and the increase in the height of the structure itself forces an enlargement of the seismic diaphragm. The period of vibrations approximates that of a structure with massive load-bearing walls, but its value is significantly reduced due to the effects discussed above. The expected period of masonry buildings according to EC-8 is $T=0.045*\text{number_of_floors}$ (s).

Seismic Period Verification it is not satisfied.

Analiza	Modi	Period	Frequency	Rotational Frequency	Cyclic Frequency	Square
		sec	cyc/sec	rad/sec	rad ² /sec ²	
Modal	1	0.058	17.342	108.9661	11873.6072	
Modal	2	0.055	18.173	114.1849	13038.1963	
Modal	3	0.051	19.632	123.3508	15215.4081	
Modal	4	0.048	20.745	130.3416	16988.9318	
Modal	5	0.045	22.323	140.2569	19671.9963	
Modal	6	0.043	23.031	144.7088	20940.643	

Table 21. The fundamental data from the modal analysis of the structure

6.2 Procedure of non-linear pushover analysis

First, the structure is modeled following the method covered in Chapter IV, which involves assigning appropriate element and material nonlinearity and utilizing the TREMURI software. A total of 24 analyses are computed for the building, incorporating various load scenarios, directions, and eccentricities.

Analysis

Control node

Level [2] Level 2 Node 54

Displacement Use weighted average displacement

No.	Compute analysis	Earthquake direction	Seismic load	Eccentricity [cm]
1	<input checked="" type="checkbox"/>	+X	Uniform	0,0
2	<input checked="" type="checkbox"/>	+X	Modal distribution	0,0
3	<input checked="" type="checkbox"/>	-X	Uniform	0,0
4	<input checked="" type="checkbox"/>	-X	Modal distribution	0,0
5	<input checked="" type="checkbox"/>	+Y	Uniform	0,0
6	<input checked="" type="checkbox"/>	+Y	Modal distribution	0,0
7	<input checked="" type="checkbox"/>	-Y	Uniform	0,0
8	<input checked="" type="checkbox"/>	-Y	Modal distribution	0,0
9	<input checked="" type="checkbox"/>	+X	Uniform	57,0
10	<input checked="" type="checkbox"/>	+X	Uniform	-57,0
11	<input checked="" type="checkbox"/>	+X	Modal distribution	57,0
12	<input checked="" type="checkbox"/>	+X	Modal distribution	-57,0
13	<input checked="" type="checkbox"/>	-X	Uniform	57,0
14	<input checked="" type="checkbox"/>	-X	Uniform	-57,0
15	<input checked="" type="checkbox"/>	-X	Modal distribution	57,0
16	<input checked="" type="checkbox"/>	-X	Modal distribution	-57,0
17	<input checked="" type="checkbox"/>	+Y	Uniform	141,0
18	<input checked="" type="checkbox"/>	+Y	Uniform	-141,0
19	<input checked="" type="checkbox"/>	+Y	Modal distribution	141,0
20	<input checked="" type="checkbox"/>	+Y	Modal distribution	-141,0
21	<input checked="" type="checkbox"/>	-Y	Uniform	141,0
22	<input checked="" type="checkbox"/>	-Y	Uniform	-141,0
23	<input checked="" type="checkbox"/>	-Y	Modal distribution	141,0
24	<input checked="" type="checkbox"/>	-Y	Modal distribution	-141,0

Figure 22. Pushover analysis cases

The 24 pushover scenarios for the building study are depicted in the figure above.

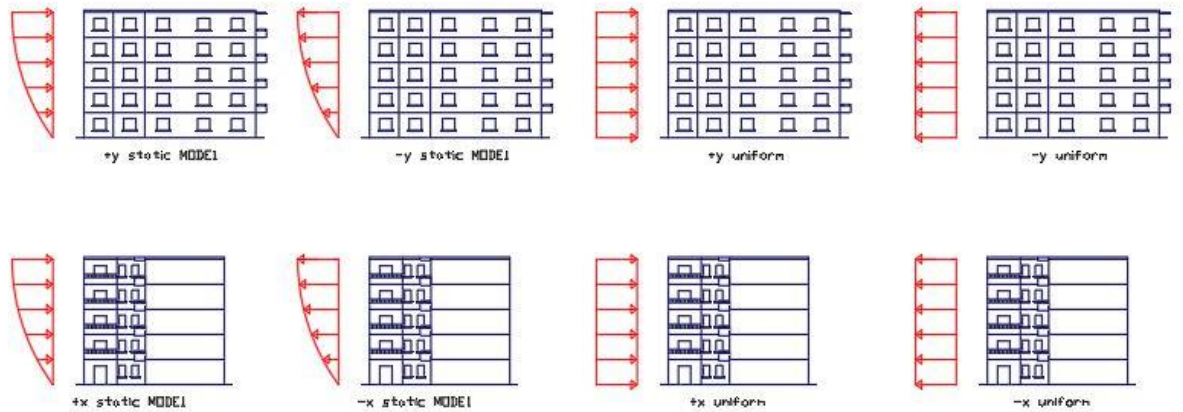


Figure 23. Load patterns and different cases of pushover analysis

The application automatically generates the analytical technique, the theoretical basis of which is provided in chapter IV. The force-displacement curve is the result of the pushover investigation in TREMURI. The worst case, or the situation with the least amount of energy dissipation, is selected as the representative capacity curve in each direction (x and y) for each of the 12 curves. After that, the curve is bilinearized using the N-2 method described in chapter IV.

No.	Seism dir.	Seismic load	Eccentricity [cm]	α NC	α SD	α DL	dm/dt NC
1	+X	Uniform	0.00	1.817	1.000	0.152	1.912
2	+X	Static forces	0.00	1.833	1.002	0.137	1.897
3	-X	Uniform	0.00	1.811	0.999	0.169	1.917
4	-X	Static forces	0.00	1.865	1.022	0.148	1.938
5	+Y	Uniform	0.00	3.110	1.726	0.220	3.863
6	+Y	Static forces	0.00	1.986	1.107	0.176	2.229
7	-Y	Uniform	0.00	2.924	1.624	0.210	3.552
8	-Y	Static forces	0.00	1.850	1.033	0.173	2.051
9	+X	Uniform	86.80	1.820	1.001	0.154	1.912
10	+X	Uniform	-86.80	1.818	1.000	0.155	1.912
11	+X	Static forces	86.80	1.834	1.003	0.137	1.897
12	+X	Static forces	-86.80	1.836	1.004	0.137	1.897
13	-X	Uniform	86.80	1.832	1.010	0.169	1.941
14	-X	Uniform	-86.80	1.789	0.987	0.169	1.894
15	-X	Static forces	86.80	1.865	1.022	0.148	1.938
16	-X	Static forces	-86.80	1.864	1.021	0.148	1.938
17	+Y	Uniform	524.50	2.294	1.284	0.213	2.711
18	+Y	Uniform	-524.50	2.125	1.192	0.208	2.493
19	+Y	Static forces	524.50	1.396	0.787	0.168	1.481
20	+Y	Static forces	-524.50	1.539	0.867	0.178	1.671
21	-Y	Uniform	524.50	2.204	1.232	0.200	2.564
22	-Y	Uniform	-524.50	2.242	1.254	0.206	2.632
23	-Y	Static forces	524.50	1.414	0.795	0.165	1.503
24	-Y	Static forces	-524.50	1.563	0.879	0.178	1.699

Figure 24. x and y- directions worst case scenario

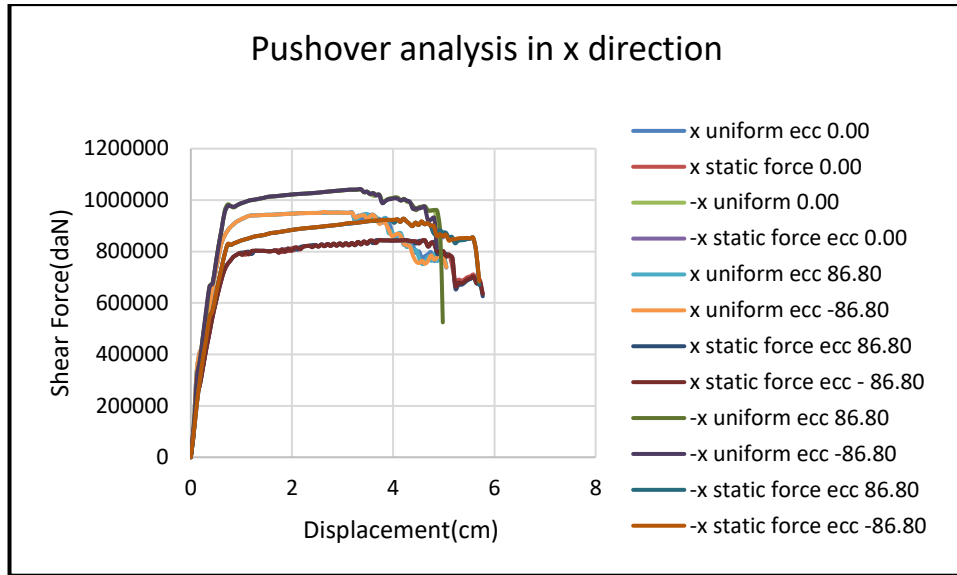


Figure 25. Pushover analysis for x-dir, 12 load patterns of case-study building

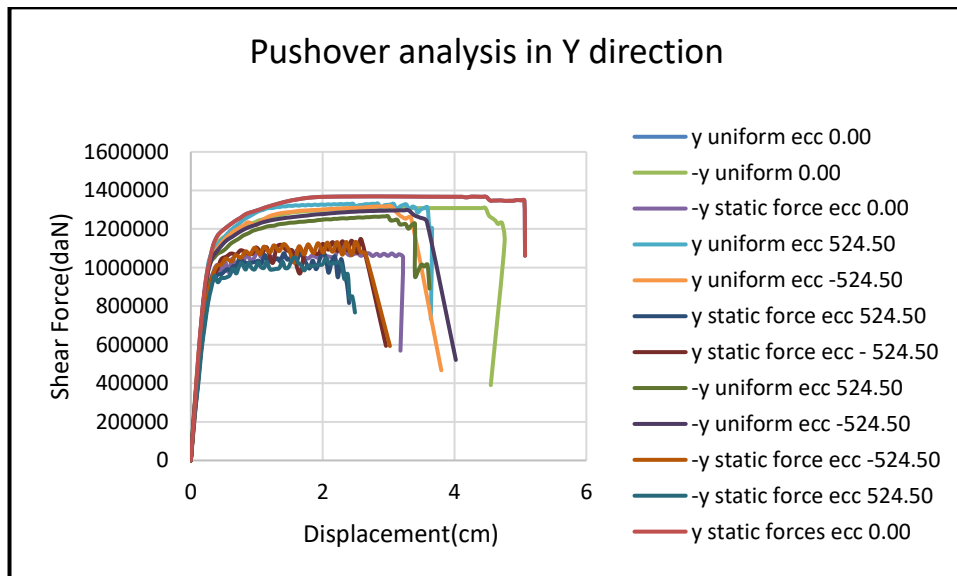


Figure 26. Pushover analysis for Y-dir, 12 load patterns of case-study building

The capacity curves are normalized and expressed in terms of the building's weight and shear force, as well as its height and top roof displacement.

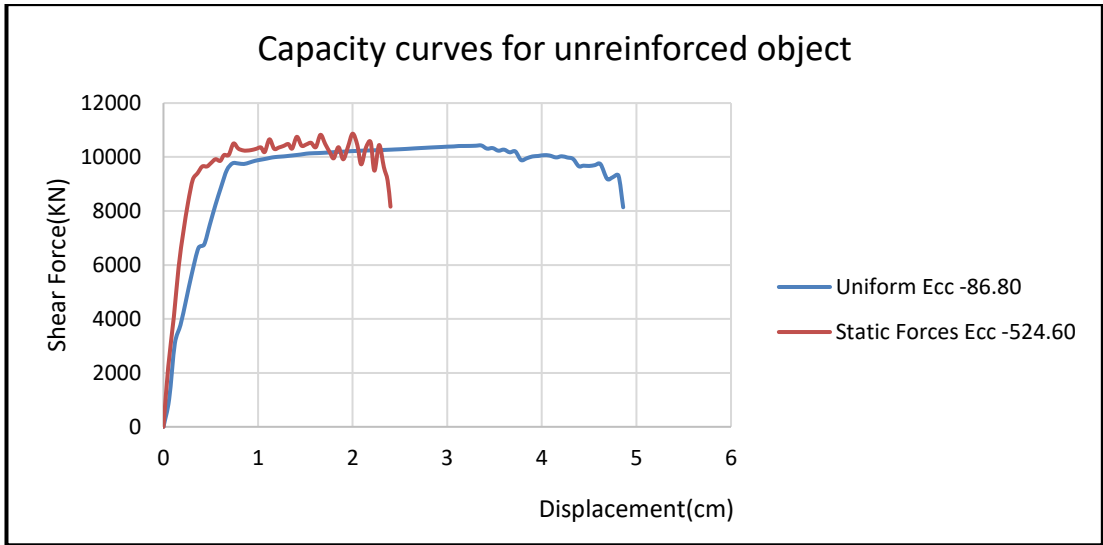


Figure 27. Capacity curve in x and y-direction, worst scenario

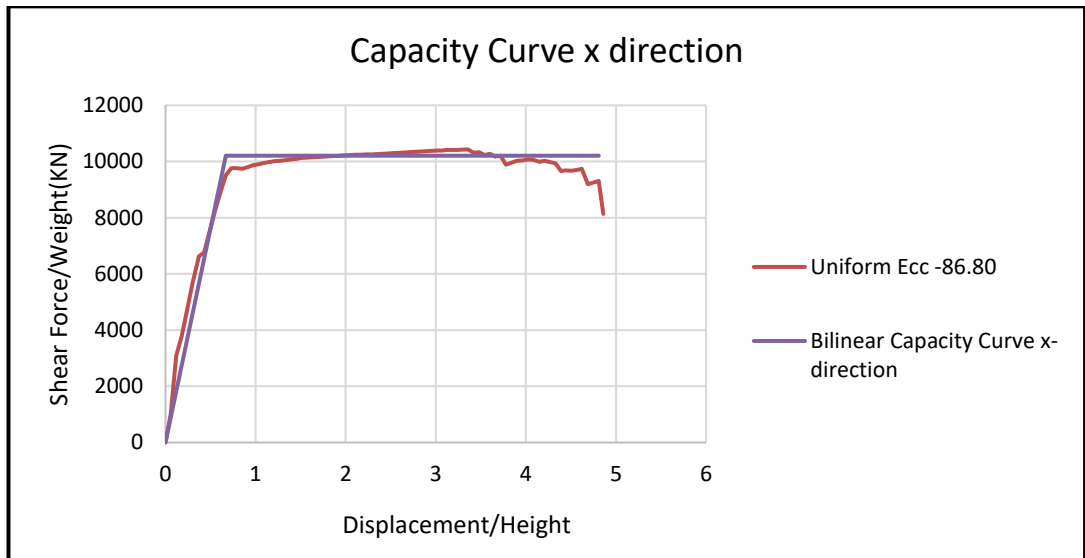


Figure 28. Normalized bilinear capacity curve in x-direction

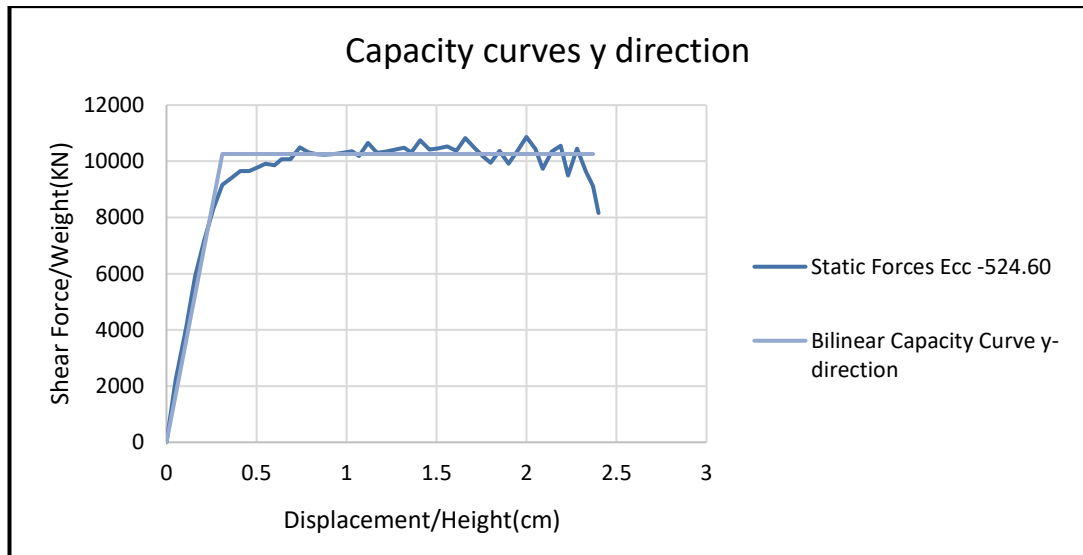


Figure 29. Normalized bilinear capacity curve in y-direction

MDOF along pushover as well as the static condition of each pier and spandel member are made possible by TREMURI. This makes it possible to create a building failure mechanism step-by-step and even regulate the anticipated degree of damage to each wall. Every limit damage condition is linked to the drift capacity of every pier and sprandel element as well as the strength and stiffness of the structure. The 24 pushover analysis cases, capacity curves in both the x and y directions, normalized capacity curves in both directions, failure mechanism, and the most laden walls for each case will be provided for each of the structures in the sections below.

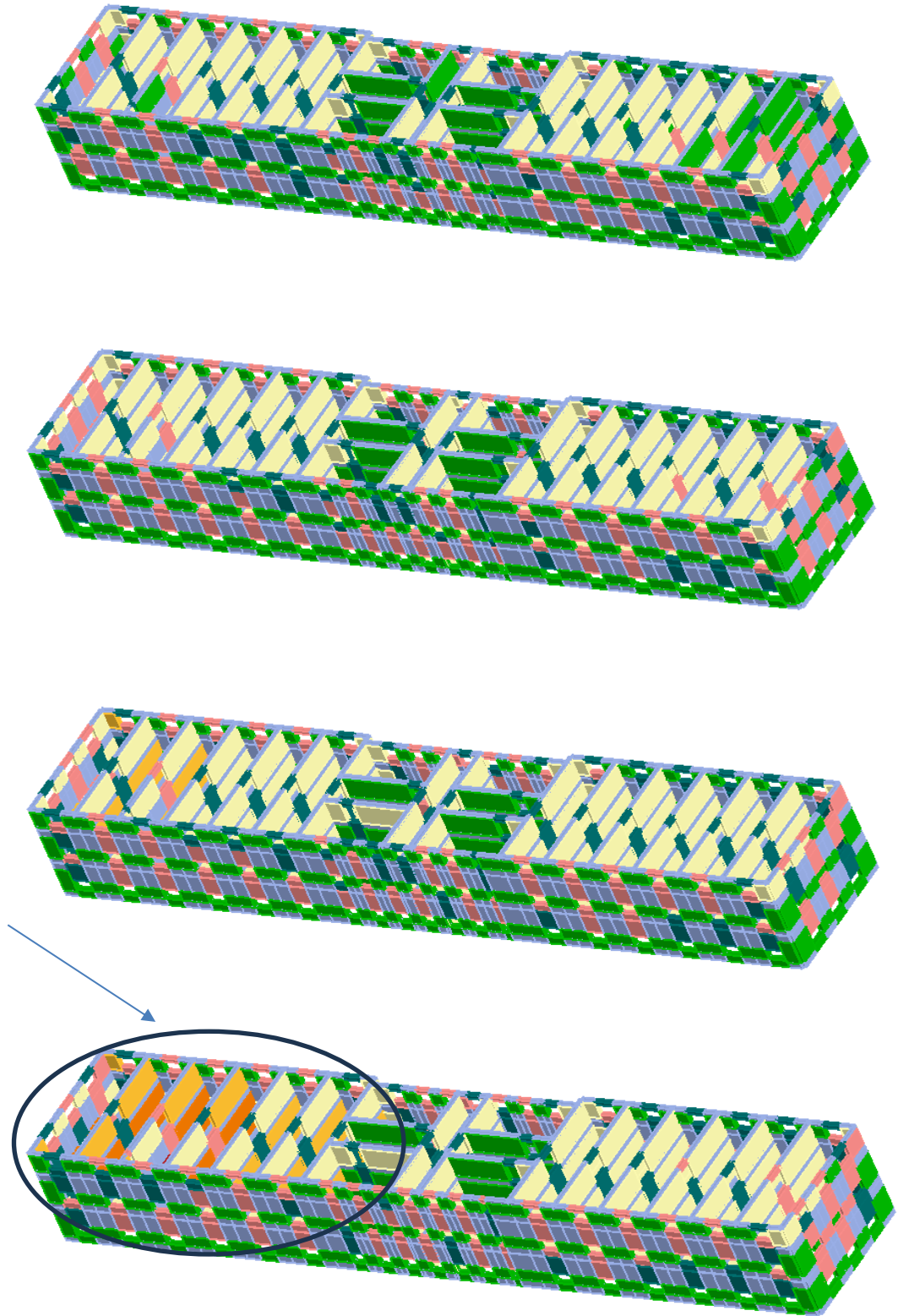


Figure 30. Most Damaged sections of the object



Figure 31. Failure mechanism

Table 22. Pushover analysis parameters of building

Load applied	d_y^*	d_m^*	F_y^*	K^*	μ	F_y^*/W
x-direction	0.67cm	4.81cm	10205.3 KN	15232kN/cm	7.18	0.5494
y-direction	0.31cm	2.37cm	10259.7 KN	33097kN/cm	7.64	0.6141

Figure 32. 3d view

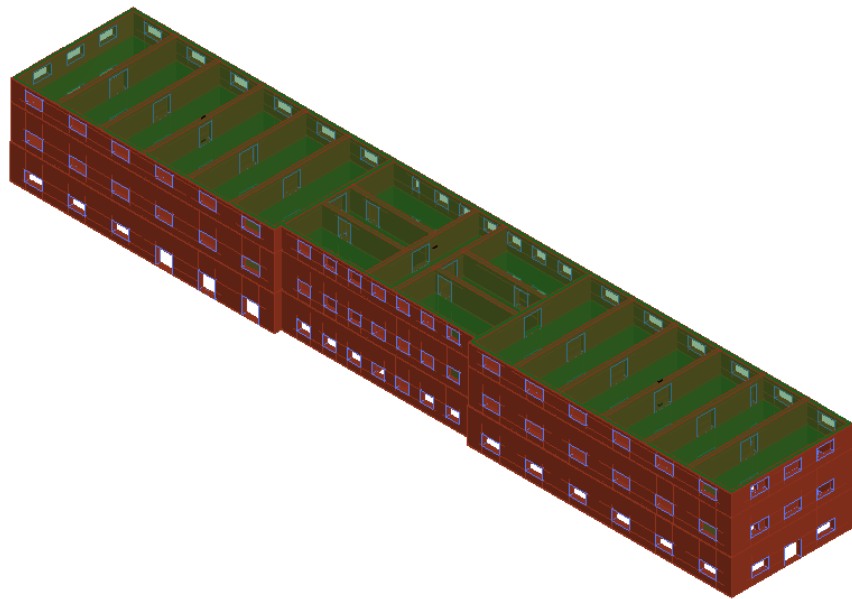


Table 23. Global displacement drift capacities (%)

Direction	(Damage Limitation (DL))	Significant Damage (SD)	Near Collapse (NC)
	$\Delta_{\text{roof}}/H_{\text{building}}$		
x	0.0000515	0.00026344	0.00037
y	0.00002385	0.000129803	0.000182308

6.3 Conclusions

After this analysis, a comparison is made between the structure's capacity and the seismic design spectrum for the conditions of non-collapse and limited damage. According to EC-8, for the structure to guarantee proper seismic performance, it must perform at the DL (Damage Limitation) level for the earthquake with a return period of 95 years, corresponding to an acceleration level $a_g=0.173g$ in our case. Similarly, for the earthquake with a return period of 475 years, with an acceleration level $a_g=0.352g$ in our case, it should perform at the SD (Significant Damage) level. The procedure followed in this case is in accordance with EC-8, comparing the capacity and earthquake in the Sa-Sd spectral format. The structure's capacity is assessed based on y , as it indicates weaker performance. In the figure below, this comparison is illustrated, showing that the structure has surpassed the DL performance level and is in the SD phase for the earthquake with a return period of 95 years, corresponding to an acceleration level $a_g=0.173g$. This implies that the structure does not meet the damage limitation condition according to EC-8. Making the same comparison, this time for the earthquake with a return period of 475 years, with an acceleration level $a_g=0.352g$, it is observed that the structure has exceeded the NC (Near Collapse) performance level, indicating it is on the brink of collapse. This means that even the non-collapse condition is not satisfied, and the structure is at risk for an earthquake with a return period of 475 years.

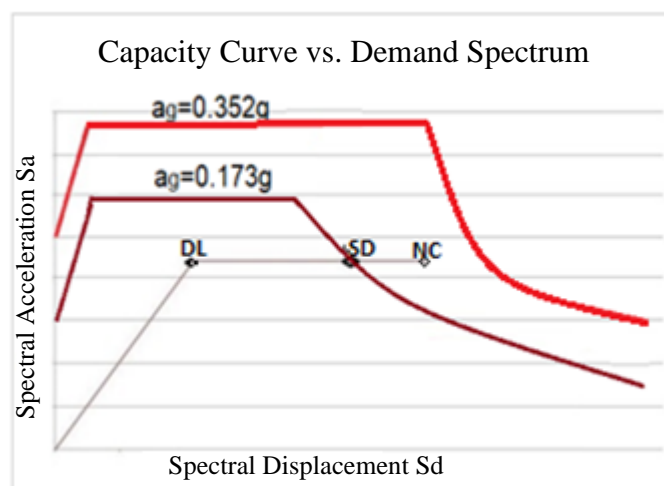


Figure 33. Capacity Curve vs. Demand Spectrum for the unreinforced object

The structure is built with load-bearing solid walls without seismic reinforcements. As such, structural damage will only consider damages to the load-bearing walls, foundations, or beams. It's worth noting that the building has a much greater longitudinal dimension than its transverse one (105.54 m versus 17.96 m). This results in the presence of the torsion phenomenon during seismic movements, causing damage in a specific part of the structure (where the two rectangular elements of the building meet). In this area, damages have been observed both in the load-bearing masonry and the floor slab. The second-floor level was added later, and the materials used for the load-bearing masonry have weaker physical and mechanical characteristics compared to the lower part. This leads to a reduction in stiffness and an increase in stresses on the walls. Additionally, the foundations are insufficient for the depth of immersion, as the building height was increased with the addition of the floor. The high presence of moisture, especially on the second floor, has caused significant degradation of materials and damage to some parts of the structure, mainly in the ceiling floors and perimeter walls. This is due to the lack or poor implementation of waterproofing in this part of the building. This problem needs to be addressed during the reconstruction of the structure. All the identified issues above need solutions, and the structure requires reinforcement.

From the conducted analyses, it was observed that the structure does not meet the conditions for limited damage and non-collapse. According to EC-8, this means that the structure needs reinforcement.

CHAPTER 7

METHODOLOGY AND PROPOSED STRENGTHENING OF EXISTING STRUCTURE

7.1 General Overview

As indicated in the previous chapter, the existing structure needs to be strengthened to increase its capacity to resist horizontal loads. Below are the necessary recommendations from the expert group to transform the existing structure into a conforming one based on technical conditions and adaptation to Albanian/Eurocode standards or other equivalent technical specifications and standards. All structural interventions in the existing building must comply with and adhere to the rules and criteria of Eurocodes. The main structural interventions to be carried out in the existing structure are as follows:

Installation of reinforced concrete columns: The columns will be installed from the foundation level to the floor slab of the last floor. They will be connected to the existing beams and concrete/steel walls as detailed in the construction project.

Strengthening of floor slabs and beams: Carbon Fiber Reinforced Polymer (CFRP) will be used to strengthen the floor slabs and beams, enhancing their load-bearing capacity.

Strengthening of load-bearing walls: Since the building has a system of massive load-bearing walls, and these walls have suffered significant damage, they will be strengthened using concrete/steel jacketing to increase their rigidity and load-bearing capacity.

Strengthening of foundations: Due to the reinforcement of columns and the addition of additional reinforced concrete walls, the reconstruction of existing foundations is envisaged in the construction project, including the addition of connecting beams. Expansion of the existing foundations will also be carried out according to rules and technical specifications.

7.2 Methodology for Repair and Strengthening of Structural Elements

Based on the assessment and analysis of existing structures and the requirements for further use of the facility, the Jacketing (concrete jacketing) method has been accepted for the repair and strengthening of structural elements. This method is applied to beams, columns, and slabs by removing damaged parts. The implementation process is as follows:

Removal of damaged parts of concrete until exposing the reinforcement bars. After removing the damaged protective layer, the process continues to expose all corroded areas of reinforcement bars, if any. The reinforcement bars must be cleaned from all sides. The space between the cleaned reinforcement bars and the existing concrete must be at least 1 cm. Care must be taken during the stripping process to avoid damaging the bond between the reinforcement bars and the concrete in unstripped areas. If these areas are damaged, they must be exposed for treatment. To ensure the bond of the new concrete with the cleaned surfaces, the application of a bonding agent is required, following the technological requirements of this material, or other materials that serve the same purpose. The filling material used for repair must have the particle size and consistency that allows easy workability and ensures uniform filling and closing of all voids in the treated area. The compressive strength of the filling material must be Class C20/25. To protect against various environmental agents, the filling material must be prepared for Exposure Class XC4. After the filling material has hardened, coating must be applied using elastic protective materials.

The pouring of the produced concrete on-site is done according to the possibilities and conditions where it will be poured. It is crucial in the process of pouring concrete into the structure to minimize the time from production to pouring to prevent the loss of its strength, workability, or consistency. Additionally, proper vibration during this process is essential. Due to its physico-mechanical characteristics, concrete vibration plays a significant role in achieving the design class or preventing various cracks. Special care should be taken during the vibration process to avoid damaging the rebars, both horizontal and vertical.

Various methods can be used for the successful implementation of repairs or reinforcements based on the specifications of the damaged elements' positions. Three different methods are proposed in this project:

- Use of formwork and traditional vibration of the repair material.
- Use of closed formwork and pumping of the repair material.
- Direct filling by pumping the repair material without using formwork.

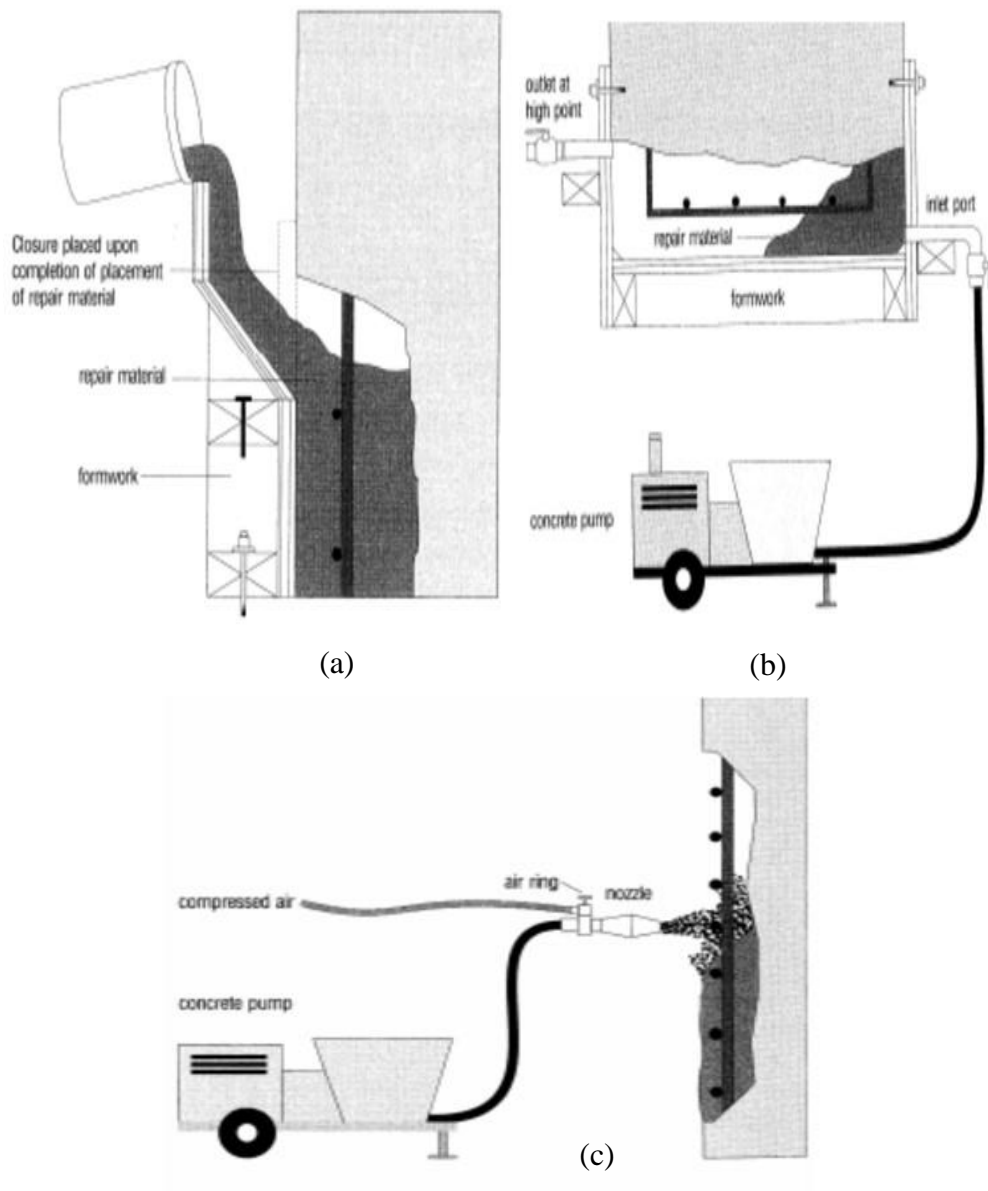


Figure 34. Different methodologies for the implementation of concrete jacketing in the structure.

For the reinforcement of walls using the Textile Reinforcement Mortar (TRM) method, the cleaning and repair process of the existing surface should involve removing plaster and all impurities until reaching a clean brick surface. Pre-wetting spray is then applied to the entire wall surface. The first layer of plaster is applied, followed by the placement of textile mesh. Finally, the second layer of plaster is applied. The reinforcement of the internal concrete of the walls (brick + concrete) will be done by injection from the sides with low-dispersion resins. The type of resins is different for masonry and concrete injections. Concrete injections will be pressure-controlled to avoid damage to degraded concrete. The characteristics and technology of the injection resins will be applied based on the specifications provided by the manufacturer.



Figure 35. *The cleaning and repair of existing surface cracks on the floor slab.*

The strengthening of the building will be realized in various ways, including the use of carbon fiber for the reinforcement of beams, the CAM system for the reinforcement of beams, columns, and walls, as well as the TRM Textile Reinforcement Mortar method for the reinforcement of walls. To reinforce the structure with carbon fibers, the application begins with a two-component epoxy resin primer to create a flat and suitable surface. This process is followed by leveling the surface with epoxy putty to avoid the formation of air gaps on the surface. Subsequently, an epoxy-based adhesive

layer is applied to create a suitable layer for bonding carbon fibers. After necessary checks, carbon fibers with a weight of $\geq 400 \text{ g/m}^2$ are applied, taking special care to avoid creating air bubbles.



Figure 36. The application of primer according to the manufacturer's specifications,



Figure 37. The placement of carbon fibers.

perimeter wall to facilitate the placement of the reinforcing columns. The columns will be supported on the existing foundation of the building reinforced with a reinforced concrete cushion. The demolition work for the column installation will not be carried out immediately but alternately and staggered. The rebars of the columns will be connected to the existing structure before their installation by opening holes with a depth of 15 cm and a diameter of $\phi 22$. Surface cleaning of the existing structure must be done before casting the columns.

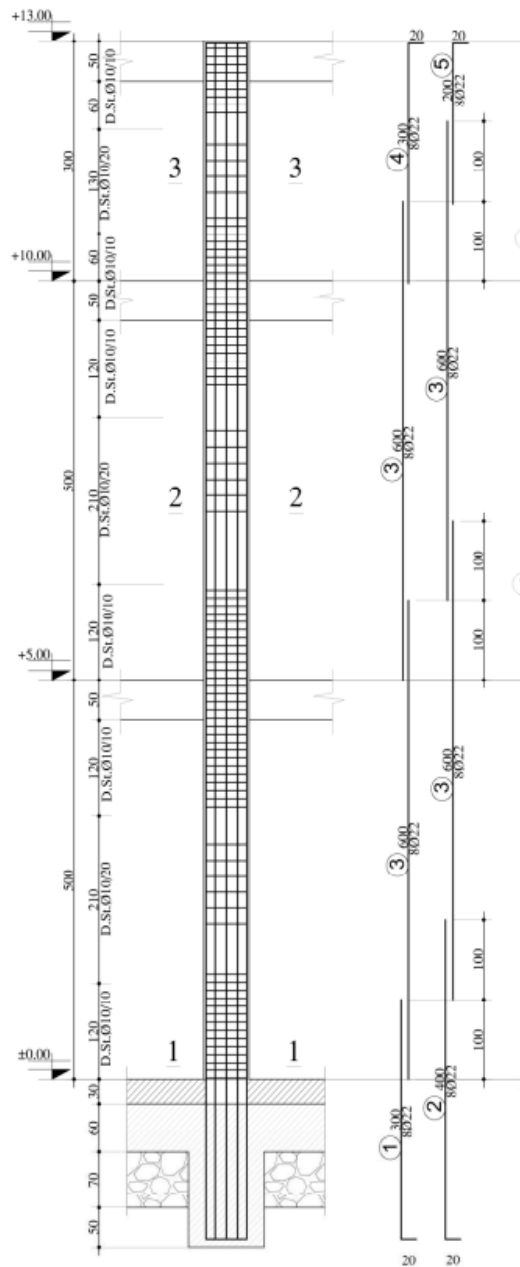


Figure 39. The details of column installation in the perimeter wall.

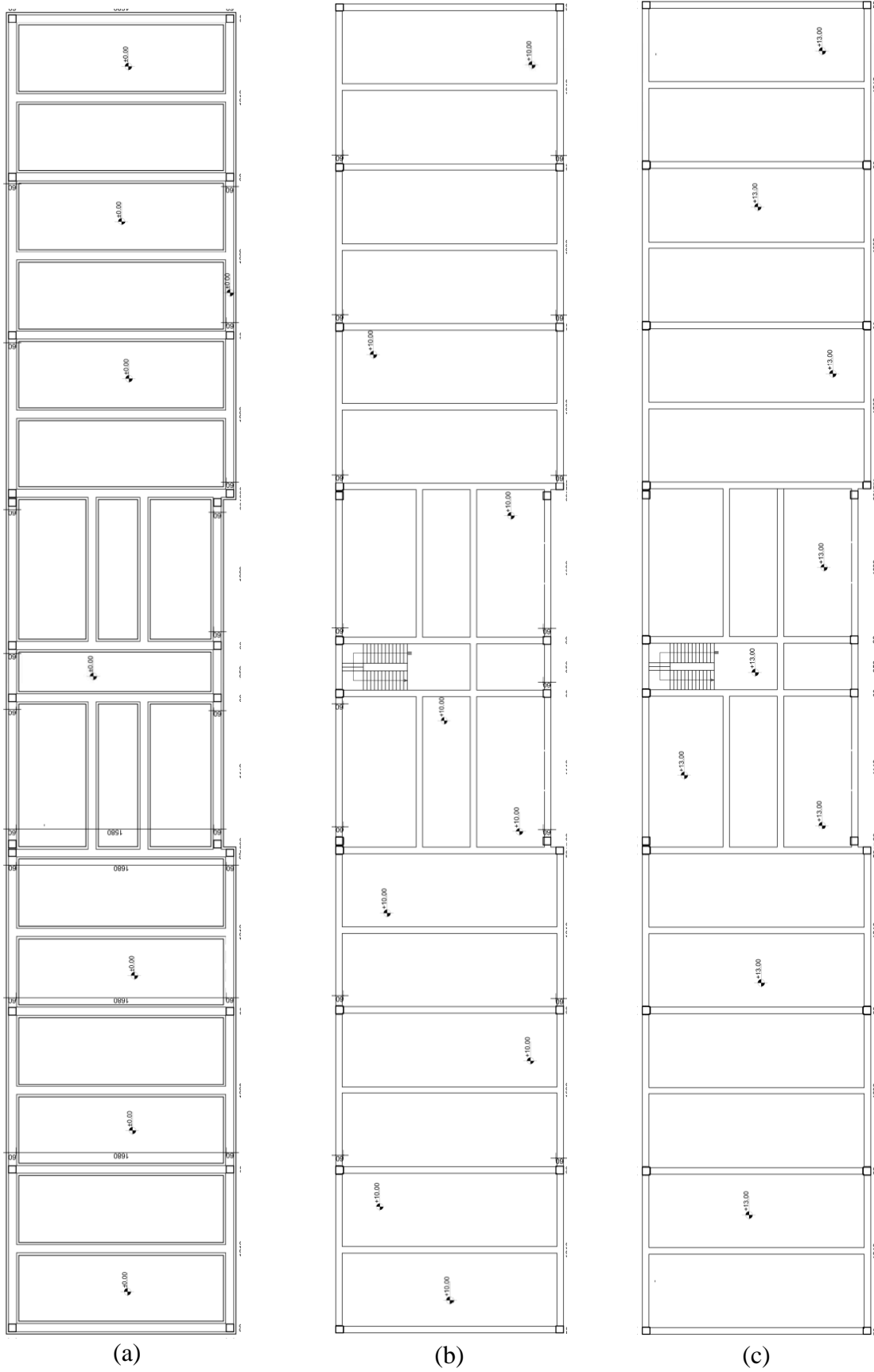


Figure 40. Reinforced plan of the three-story structures.

Perimeter walls will also be reinforced with concrete/steel jacketing with steel mesh $\phi 12$ at intervals of 15 cm. The walls will also be constructed with C20/25 concrete and S450 steel. Detailed specifications are also provided in the construction project.

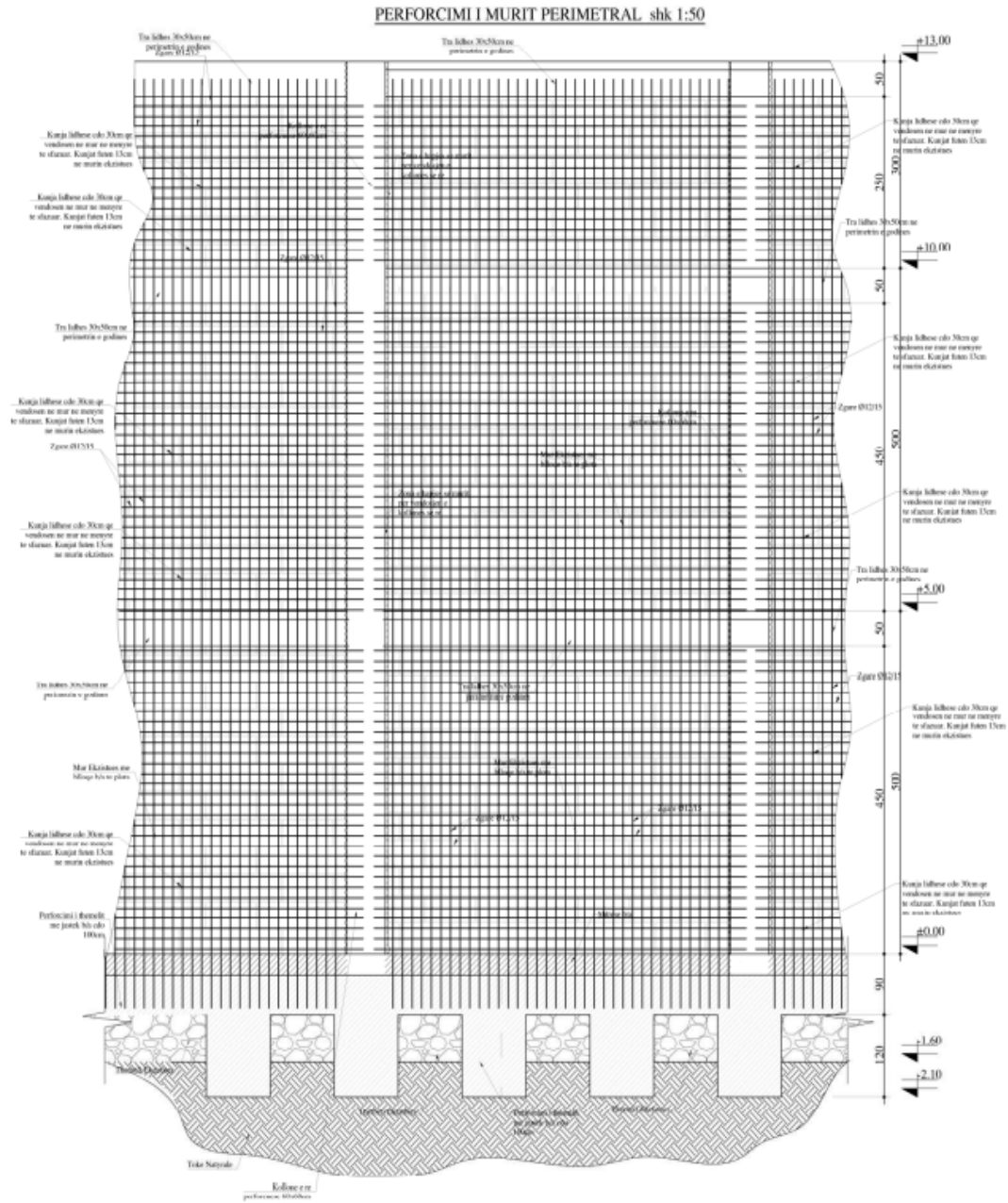


Figure 41. Reinforcement of the perimeter wall with steel mesh.

The floor slabs have been reinforced with carbon fibers CFRP, as discussed earlier. Data are provided in the construction project and technical specifications.

CHAPTER 8

OUTPUTS OF THE ANALYSES OF THE REINFORCED OBJECT

MDOF along pushover as well as the static condition of each pier and spandel member are made possible by TREMURI. This makes it possible to create a building failure mechanism step-by-step and even regulate the anticipated degree of damage to each wall. Every limit damage condition is linked to the drift capacity of every pier and sprandel element as well as the strength and stiffness of the structure. The 24 pushover analysis cases, capacity curves in both the x and y directions, normalized capacity curves in both directions, failure mechanism, and the most laden walls for each case will be provided for each of the structures in the sections below.

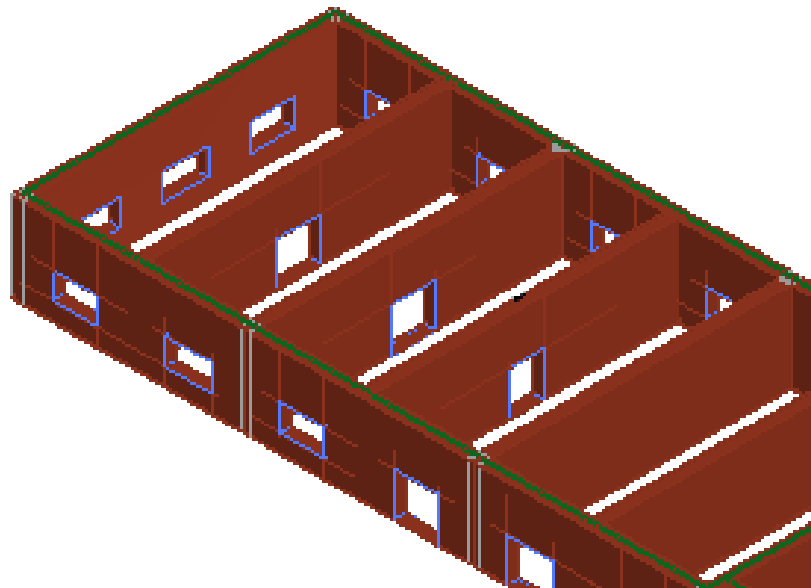


Figure 43. Close view of the column Insertion

No.	Seism dir.	Seismic load	Eccentricity [cm]	α NC	α SD	α DL	dm/dt NC
1	+X	Uniform	0.00	2.190	2.101	1.568	2.408
2	+X	Static forces	0.00	2.175	2.079	1.398	2.347
3	-X	Uniform	0.00	2.114	2.035	1.735	2.341
4	-X	Static forces	0.00	2.294	2.193	1.514	2.500
5	+Y	Uniform	0.00	2.342	2.196	3.124	2.912
6	+Y	Static forces	0.00	2.373	2.315	2.550	2.923
7	-Y	Uniform	0.00	2.023	1.956	2.894	2.476
8	-Y	Static forces	0.00	2.344	2.280	2.364	2.837
9	+X	Uniform	86.80	2.192	2.103	1.572	2.408
10	+X	Uniform	-86.80	2.189	2.100	1.568	2.404
11	+X	Static forces	86.80	2.194	2.097	1.396	2.367
12	+X	Static forces	-86.80	2.194	2.096	1.394	2.367
13	-X	Uniform	86.80	2.113	2.034	1.735	2.341
14	-X	Uniform	-86.80	2.114	2.035	1.737	2.341
15	-X	Static forces	86.80	2.275	2.176	1.514	2.479
16	-X	Static forces	-86.80	2.293	2.193	1.516	2.500
17	+Y	Uniform	524.50	2.102	1.971	2.784	2.420
18	+Y	Uniform	-524.50	3.557	3.335	3.200	4.496
19	+Y	Static forces	524.50	2.578	2.435	2.316	3.044
20	+Y	Static forces	-524.50	1.876	1.845	2.442	2.209
21	-Y	Uniform	524.50	1.808	1.744	2.568	2.082
22	-Y	Uniform	-524.50	6.287	5.894	3.098	7.899
23	-Y	Static forces	524.50	2.392	2.316	2.122	2.821
24	-Y	Static forces	-524.50	1.714	1.692	2.420	1.982

Figure 44. *x* and *y* worst case scenario for the reinforced object

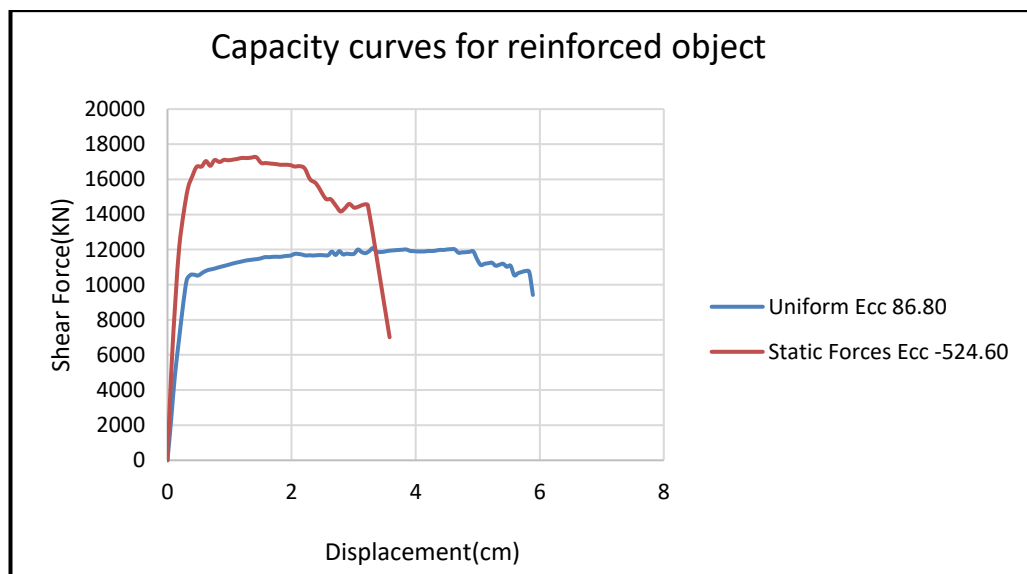


Figure 45. *Capacity curve in x and y-direction, worst scenario*

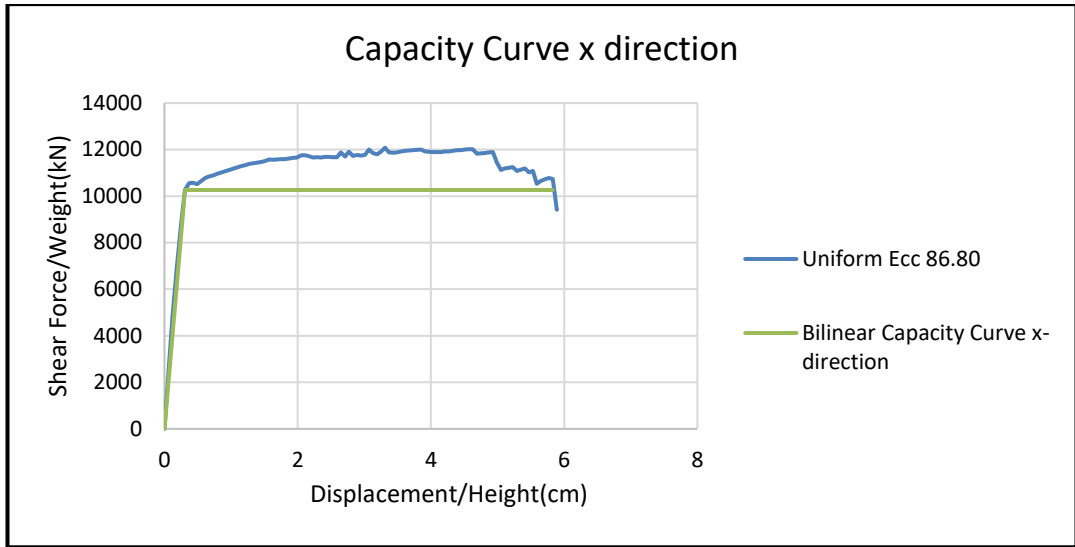


Figure 46. Normalized bilinear capacity curve in x-direction

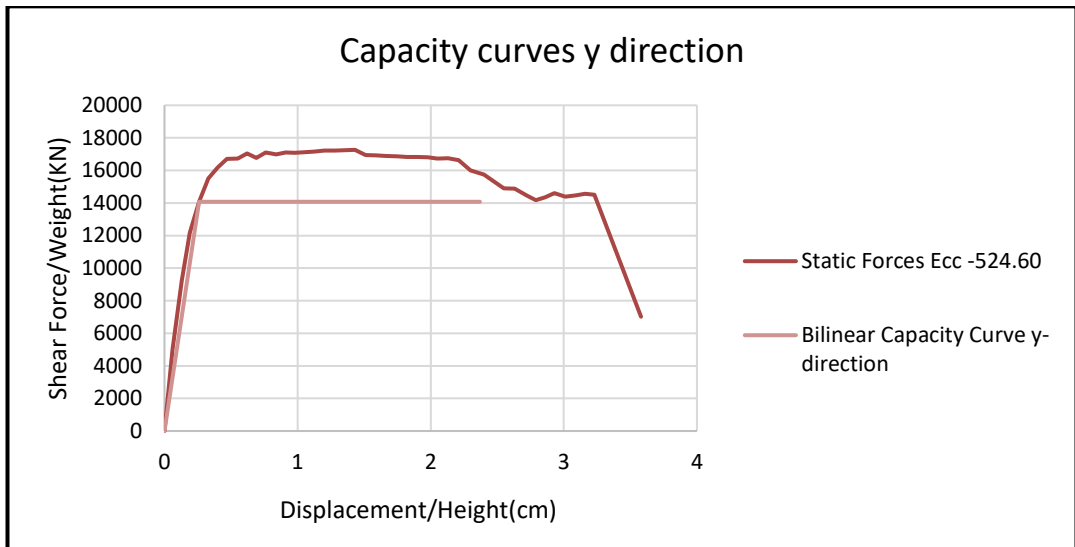


Figure 47. Normalized bilinear capacity curve in y-direction

CHAPTER 9

CONCLUSIONS

9.1 Conclusions

In seismic terms, as shown earlier, the structure was in the NC phase according to EC-8 after the earthquake. After the intervention, for a seismic event with a return period of 475 years, the building is guaranteed not to reach the SD state. Moreover, the condition of limited damage is ensured for the building, given that it is in the DL phase, for a seismic event with a return period of 95 years.

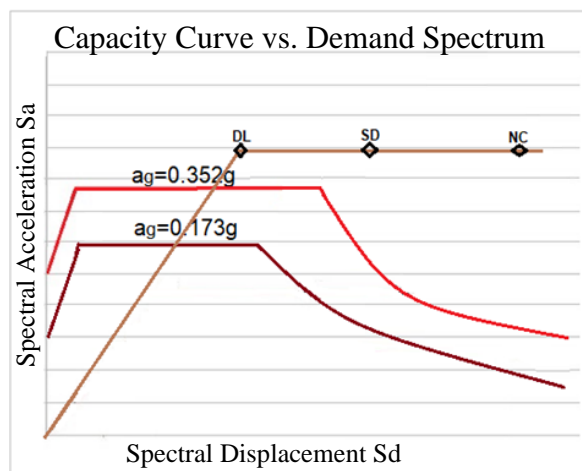


Figure 48. Comparison of structure capacity with earthquake spectrum

9.2 Comparison of Structural Capacity Before and After Reinforcement

Undoubtedly, the building after the intervention exhibits increased capacity against both horizontal and vertical loads. The primary reasons, as mentioned earlier, include interventions such as:

- Strengthening of the structure's foundations
- Construction of a complete frame around columns for the structure
- Reinforcement of load-bearing walls
- Strengthening of the floor slab with CFRP fibers

Building	Max Force/Weight		Stiffness		Ductility	
	X	Y	X	Y	X	Y
Before Reinforcement.	55.16 %	24.74 %	8438 kN/m	7830 kN/m	2.54	3.78
After Reinforceemnt.	67.73 %	53.38 %	14014 kN/m	12914 kN/m	3.75	4.73

Table 24. Comparison of global mechanical characteristics of the building before and after reinforcement

In terms of maximum horizontal load-bearing force, the structure's capacity has increased by over 100% (from 0.25 to 0.53) in the Y direction, which was initially more problematic. Additionally, stiffness has significantly increased, with values rising by around 70% (from 7830 to 12914) in both directions.

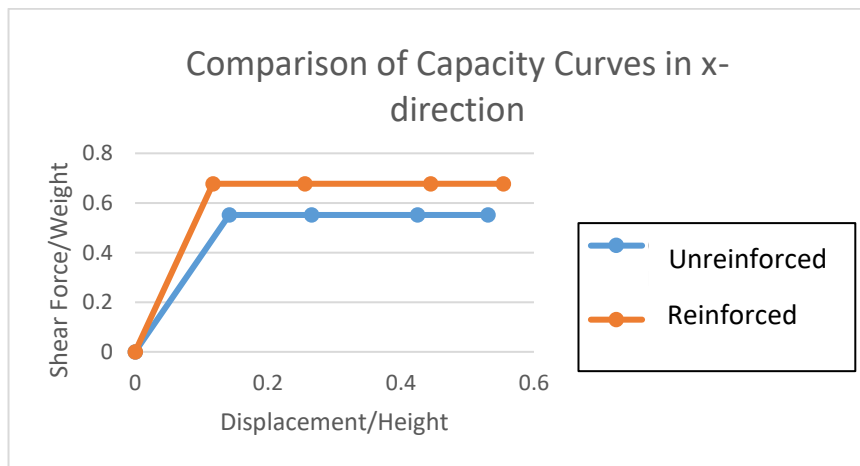


Figure 49. Comparison of capacity curves in the X direction

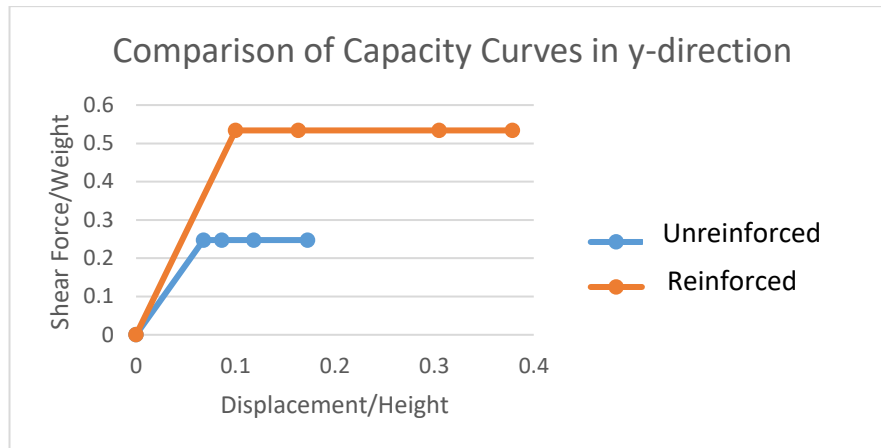


Figure 50. Comparison of capacity curves in the Y direction

9.3 Recommendations for future research

For future assessments, conducting a pushover analysis in TREMURI using the Finite Element Method (FEM) with consideration for both material and geometrical non-linearity holds promise. This approach aims to refine capacity curves and, more importantly, understand the damage patterns by comparing them with equivalent frame models. This can contribute significantly to the methodological analysis of irregular buildings or clusters.

Moreover, there is room for improvement in methodologies and tools for modeling the overall structural behavior. Enhancements in these areas will further enhance our understanding and predictive capabilities in the realm of structural engineering. Implementing the reinforcement of load-bearing walls and the strengthening of the floor slab with CFRP fibers becomes impossible in such programs so more studies should be carried out.

REFERENCES

1. Vittori, E., et al., *Geological effects and tectonic environment of the 26 November 2019, M w 6.4 Durrës earthquake (Albania)*. Geophysical Journal International, 2021. **225**(2): p. 1174-1191.
2. Bilgin, H., et al., *Reflections from the 2019 Durrës Earthquakes: An Earthquake Engineering Evaluation for Masonry Typologies*. Buildings, 2023. **13**(9): p. 2227.
3. Roberts, J. and O. Brooker, *How to Design Masonry Structures Using Eurocode 6: Introduction to Eurocode 6*. 2007: Concrete Centre.
4. Bisch, P., et al., *Eurocode 8: seismic design of buildings worked examples*. Luxembourg: Publications Office of the European Union, 2012.
5. Bilgin, H. and E. Huta, *Earthquake performance assessment of low and mid-rise buildings: Emphasis on URM buildings in Albania*. Earthquakes and Structures, 2018. **14**(6): p. 599-614.
6. Albania, C.I.o., *"Report of investigation and casualties of 26 November earthquake"*. Tirane, 2020.
7. Tomazevic, M., *Earthquake-resistant design of masonry buildings*. Vol. 1. 1999: World Scientific.
8. D'Ayala, D. and E. Speranza, *Definition of collapse mechanisms and seismic vulnerability of historic masonry buildings*. Earthquake spectra, 2003. **19**(3): p. 479-509.
9. Mustafaraj, E., *External shear strengthening of unreinforced damaged masonry walls*. 2016.
10. Alecci, V., et al., *Shear strength of brick masonry walls assembled with different types of mortar*. Construction and Building Materials, 2013. **40**: p. 1038-1045.
11. Hysenlliu, M., *Vulnerability Assessment of Current Masonry Building Stock in Albania*. 2021, EPOKA University, 2021-01-27.
12. Corradi, M., A. Borri, and A. Vignoli, *Strengthening techniques tested on masonry structures struck by the Umbria–Marche earthquake of 1997–1998*. Construction and building materials, 2002. **16**(4): p. 229-239.
13. Sitole, A., S. Guha, and S.S. Shekhawat, *CONVERSION OF MDOF SYSTEM INTO SDOF SYSTEM OF RC WAFFLE SLAB STRUCTURE BY USING N2 METHOD*. 2018.

14. Penna, A., et al. *Seismic assessment of masonry structures by non-linear macro-element analysis*. in *IV international seminar on structural analysis of historical construction-possibilities of numerical and experimental techniques*. 2004.
15. De Luca, F., D. Vamvatsikos, and I. Iervolino, *Near-optimal piecewise linear fits of static pushover capacity curves for equivalent SDOF analysis*. *Earthquake engineering & structural dynamics*, 2013. **42**(4): p. 523-543.
16. H., H.M.B.A.B., "*Analiza e performances e ndërtesave muraturë me dhe pa ndërhyrje*", "*Buletini I Shkencave Teknike*". Universiteti Politeknik I Tiranës (2020).
17. Assembly, I.t.G., *Principles for the analysis, conservation and structural restoration of architectural heritage*. Victoria Falls, Zimbabwe, 2003.
18. Belmouden, Y. and P. Lestuzzi, *An equivalent frame model for seismic analysis of masonry and reinforced concrete buildings*. *Construction and building materials*, 2009. **23**(1): p. 40-53.
19. Lagomarsino, S., et al., *TREMURI program: an equivalent frame model for the nonlinear seismic analysis of masonry buildings*. *Engineering structures*, 2013. **56**: p. 1787-1799.
20. Penna, A., S. Lagomarsino, and A. Galasco, *A nonlinear macroelement model for the seismic analysis of masonry buildings*. *Earthquake Engineering & Structural Dynamics*, 2014. **43**(2): p. 159-179.
21. Asteris, P.G., et al., *Numerical modeling of historic masonry structures*, in *Civil and Environmental Engineering: Concepts, Methodologies, Tools, and Applications*. 2016, IGI Global. p. 27-68.
22. Matysek, P. *The influence of slenderness on capacity of masonry walls*. in *Proceedings of 10th Canadian Masonry Symposium, Banff, Alberta*. 2005.
23. Hysenlliu, M. and A. Bidaj, *O 31. EVALUATION OF CAPACITY AND SEISMIC PERFORMANCE OF BRICK MASONRY BUILDINGS WITH AND WITHOUT STRUCTURAL INTERVENTIONS*.
24. Akademia e Shkencave, T., *KTP-N.2-89 Kushtet teknike të projektimit për Ndërtimet Antisizmike*,.
25. Hysenlliu, M. and E. Deneko, *Capacity Evaluation and Spectral Analysis of Damaged Low-Rise Reinforced Concrete Building*. *Journal of Transactions in Systems Engineering*, 2023. **1**(3): p. 120-130.
26. IGJEUM, "*Tërmeti I Durrësit I 26 Nëntorit 2019*". Tiranë (2020).

APPENDICES



